

## SUPPLEMENTARY INFORMATION

### Detection of free chlorine in water using graphene-like carbon based chemiresistive sensors

Ana Zubiarraín-Laserna,<sup>a</sup> Shayan Angizi,<sup>a</sup> Md Ali Akbar,<sup>a</sup> Ranjith Divigalpitiya,<sup>b</sup> Ponnambalam Ravi Selvaganapathy<sup>c</sup> and Peter Kruse<sup>\*a</sup>

<sup>a</sup>Department of Chemistry and Chemical Biology, McMaster University, 1280 Main Street West, Hamilton, Ontario L8S 4M1, Canada

<sup>b</sup>3M Canada Company, 1840 Oxford Street, London, Ontario N5V 3R6, Canada

<sup>c</sup>Department of Mechanical Engineering, McMaster University, 1280 Main Street West, Hamilton, Ontario L8S 4L7, Canada

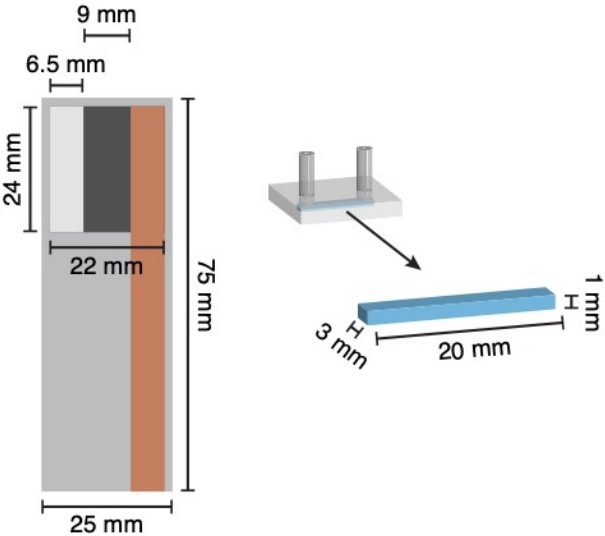
\*Corresponding Author: [pkruise@mcmaster.ca](mailto:pkruise@mcmaster.ca)

### Table of Contents

<b>Figure S1.</b> (a) Dimensions of the sensor components and the flow channel. (b) Experimental setup .....	Page S - 1
<b>Figure S2.</b> Raw data from the chemiresistive sensing characteristics as a function of GLC film thickness .....	Page S - 2
<b>Table S1.</b> Equations of the models used to fit the data in Figure S2, as well as the curve parameters obtained with each of the sensors.....	Page S - 16
<b>Figure S3.</b> Calibration curves obtained with the raw data in Figure S2, fitted to a Langmuir adsorption isotherm using the curve parameters in Table S1 .....	Page S - 18
<b>Equation S1.</b> Derivation showing that $1/B$ is proportional to the saturation concentration .....	Page S - 22
<b>Figure S4.</b> Replicates of the low range detection data.....	Page S - 23
<b>Table S2.</b> Curve parameters from the low range detection data .....	Page S - 24
<b>Figure S5.</b> Replicates of the detection of free chlorine concentration fluctuations (raw and processed data).....	Page S - 25
<b>Figure S6.</b> Replicate data from the real drinking water testing .....	Page S - 27

**Figure S1.** (a) Dimensions of the sensor components and the flow channel. The exposed area of the GLC in the dip sensors after masking the contacts with PDMS is approximately  $8 \times 22$  mm. (b) Experimental setup for measurement.

(a)



(b)

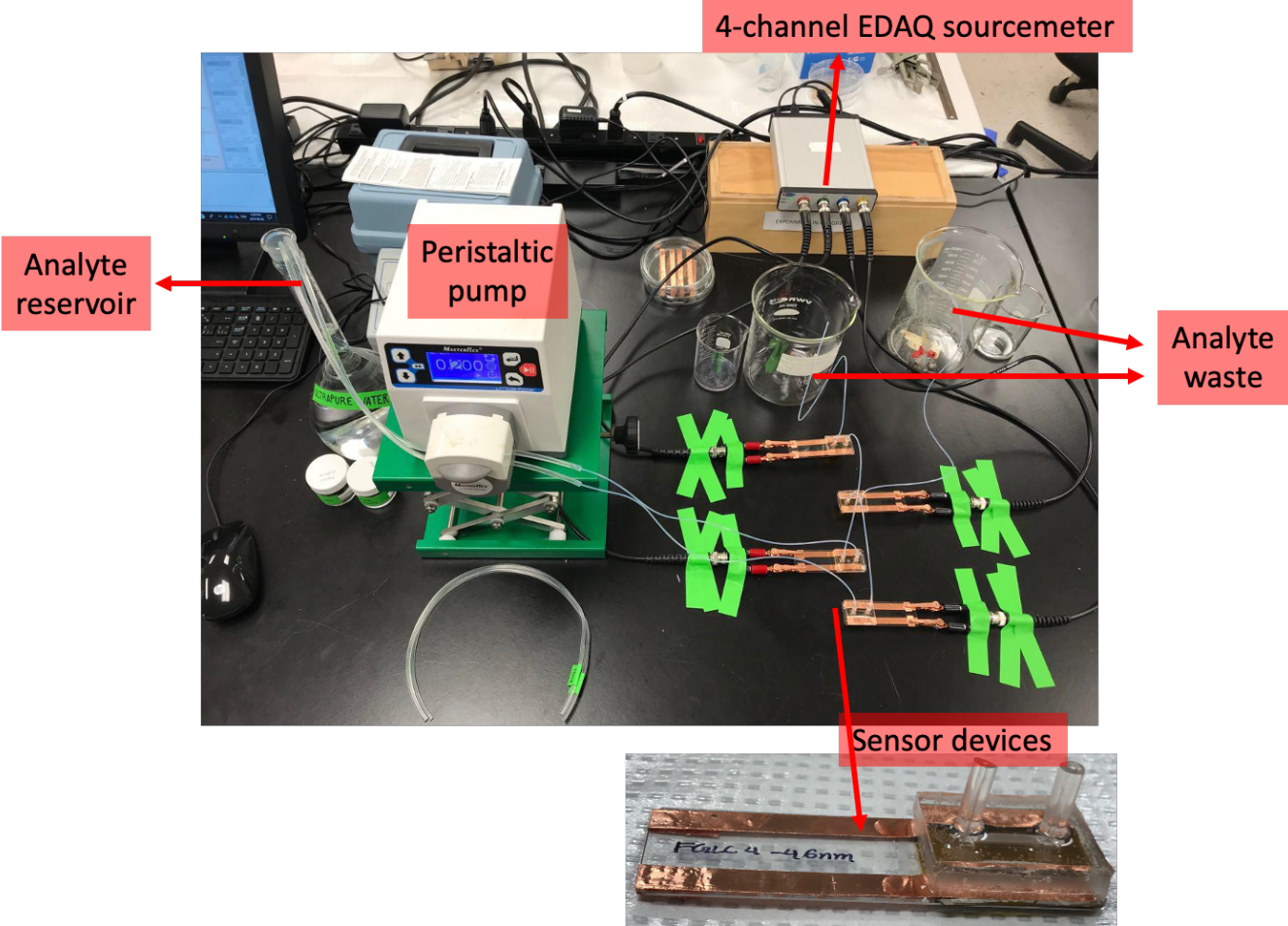
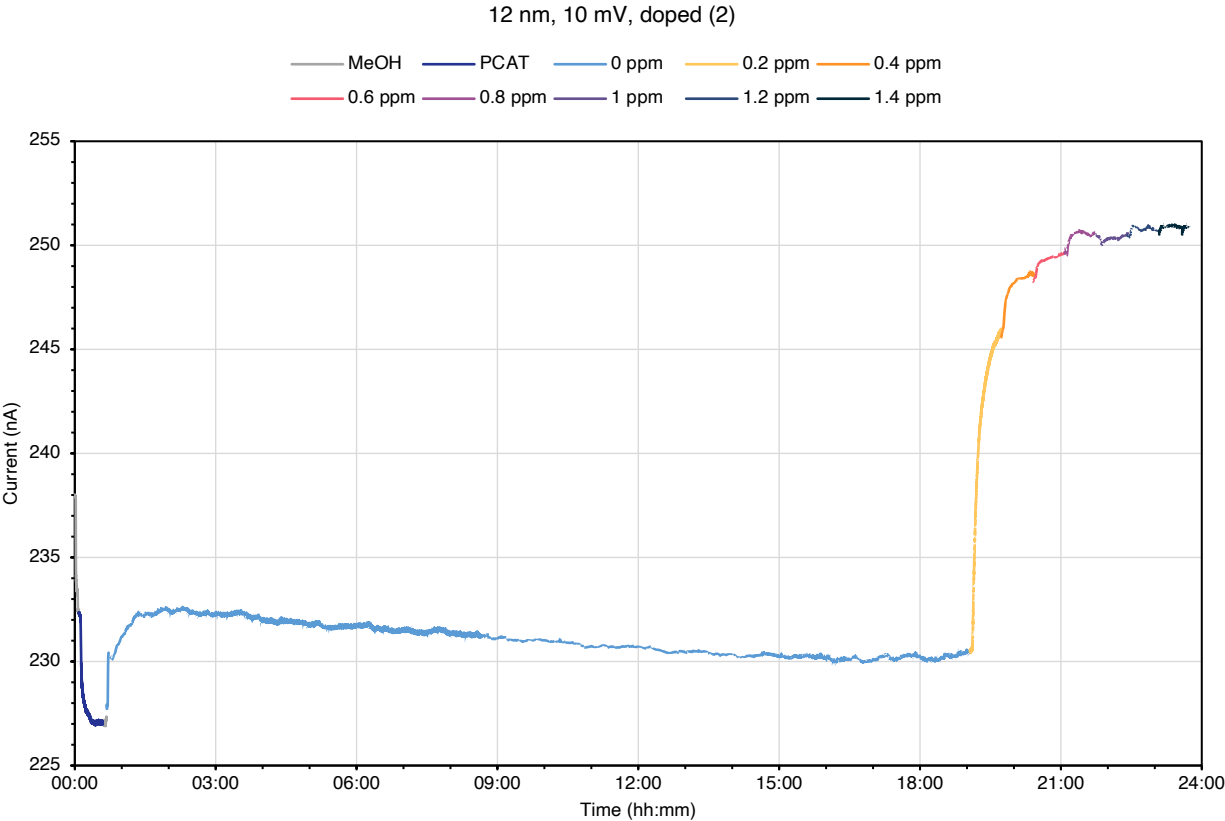
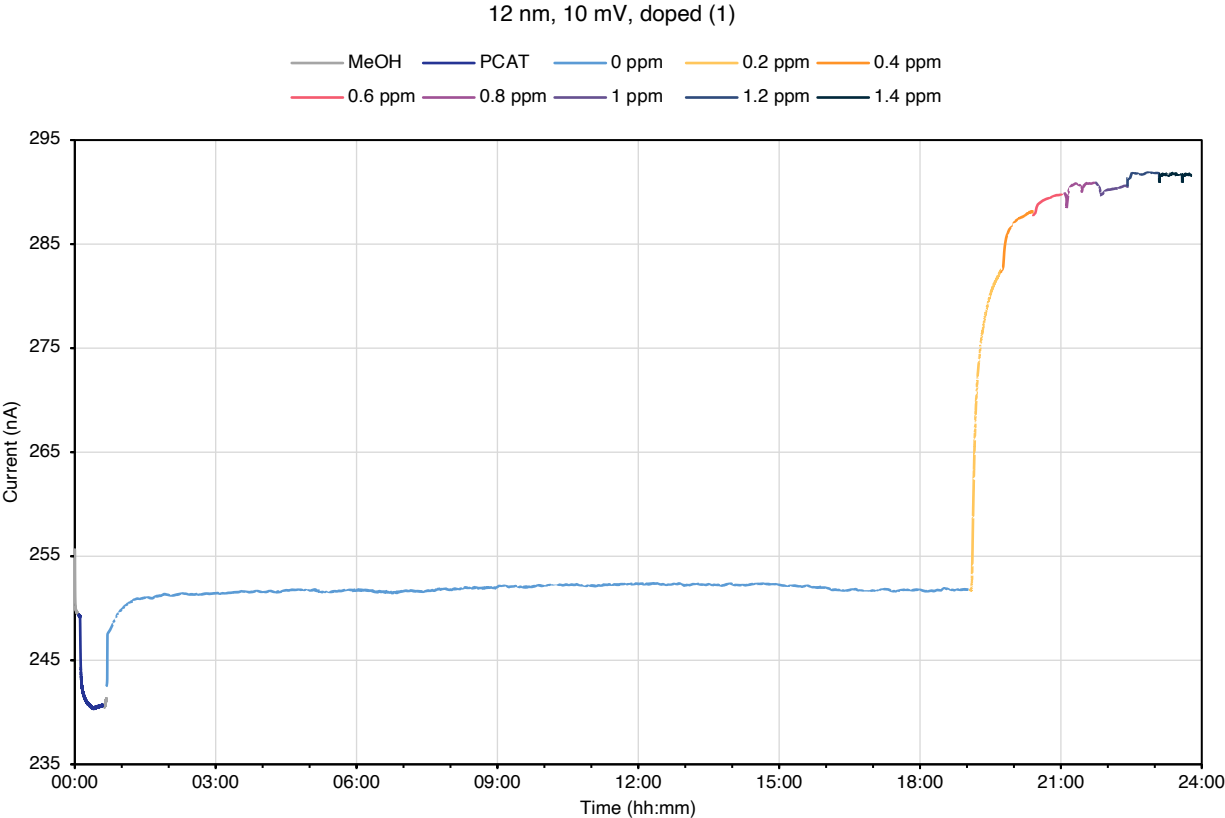
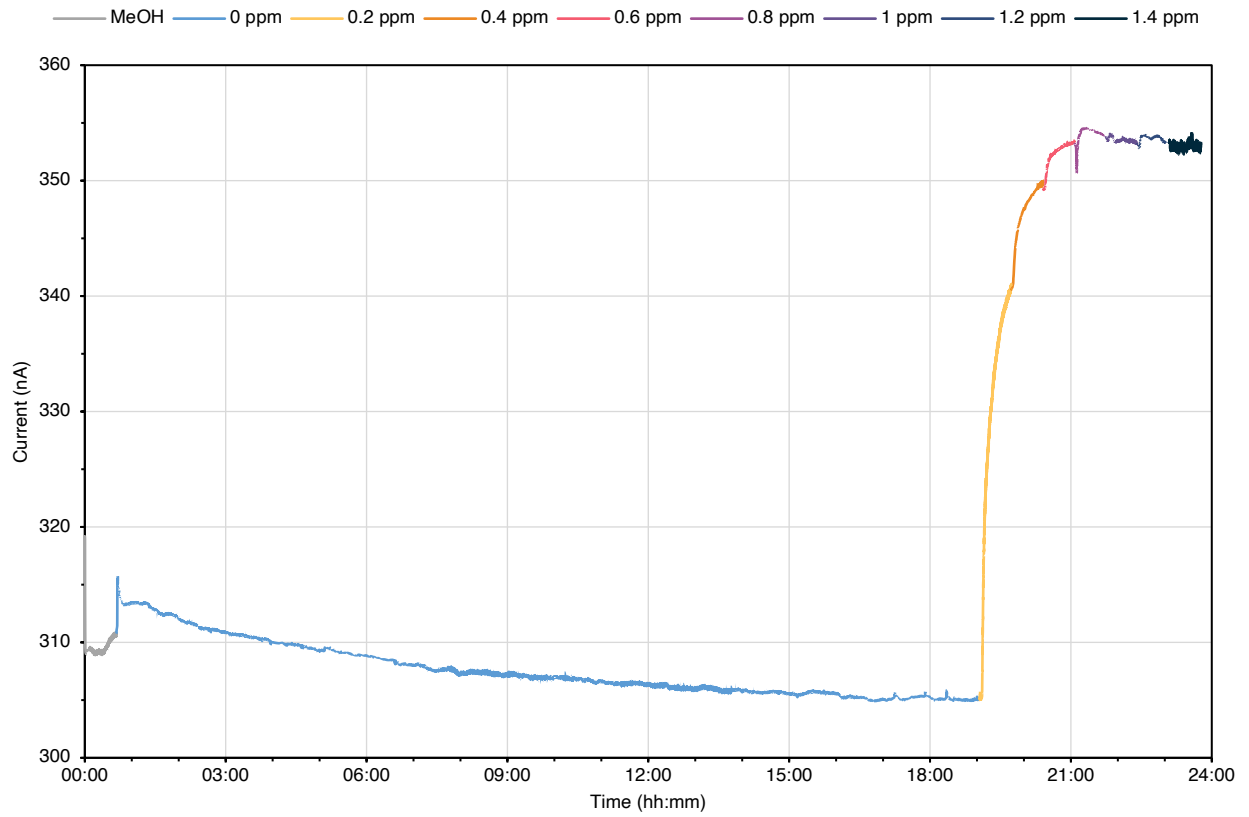


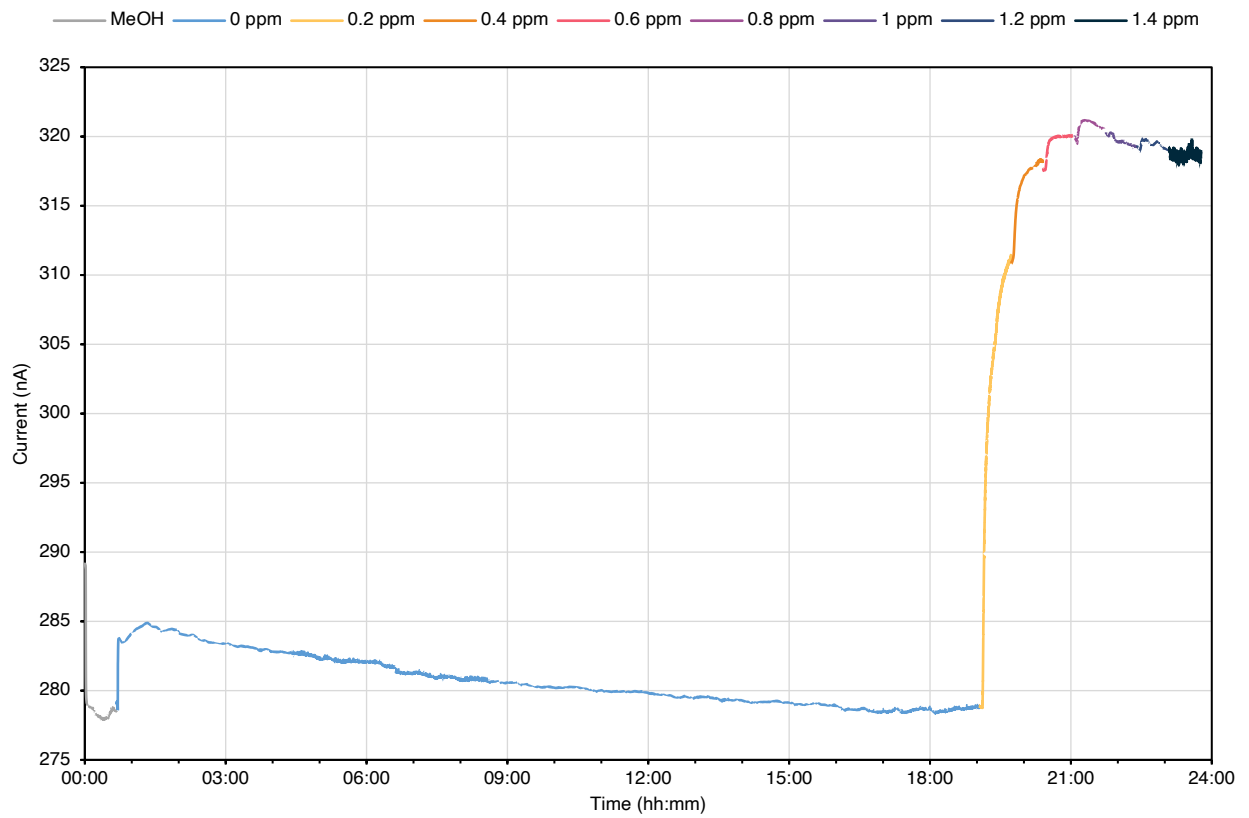
**Figure S2.** Raw data from the chemiresistive sensing characteristics as a function of GLC film thickness. The data consists of 2 doped sensors and 2 blank sensors for each thickness (i.e. 12, 24, 38, and 46 nm) and each bias (i.e. 10 mV and 100 mV).



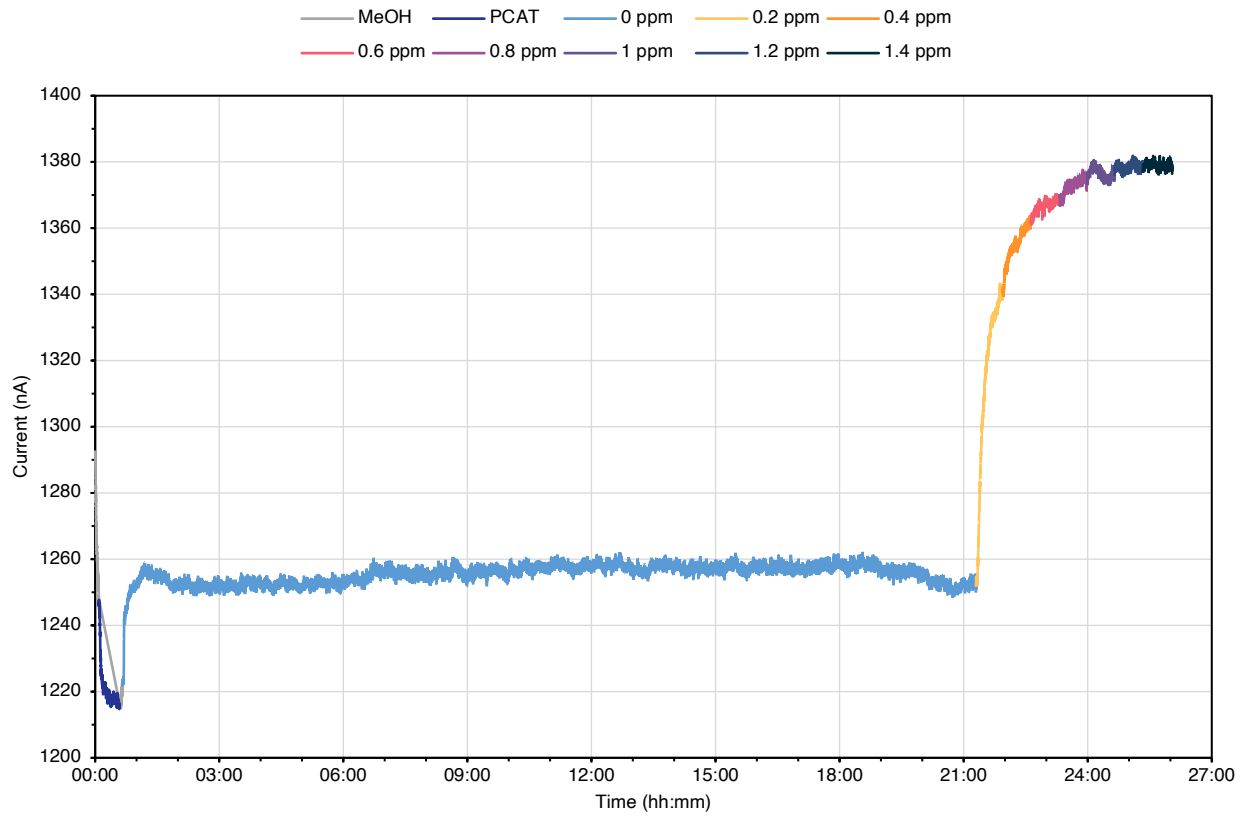
12 nm, 10 mV, blank (1)



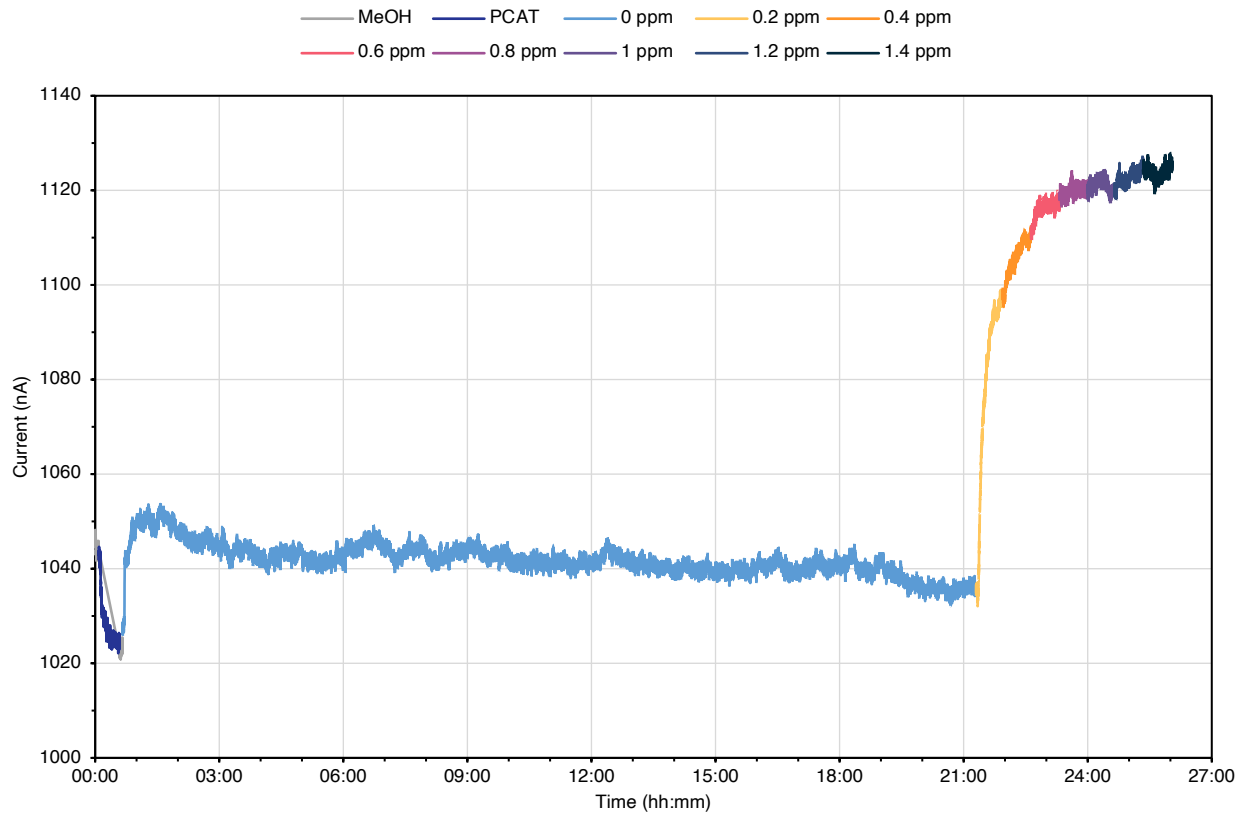
12 nm, 10 mV, blank (2)



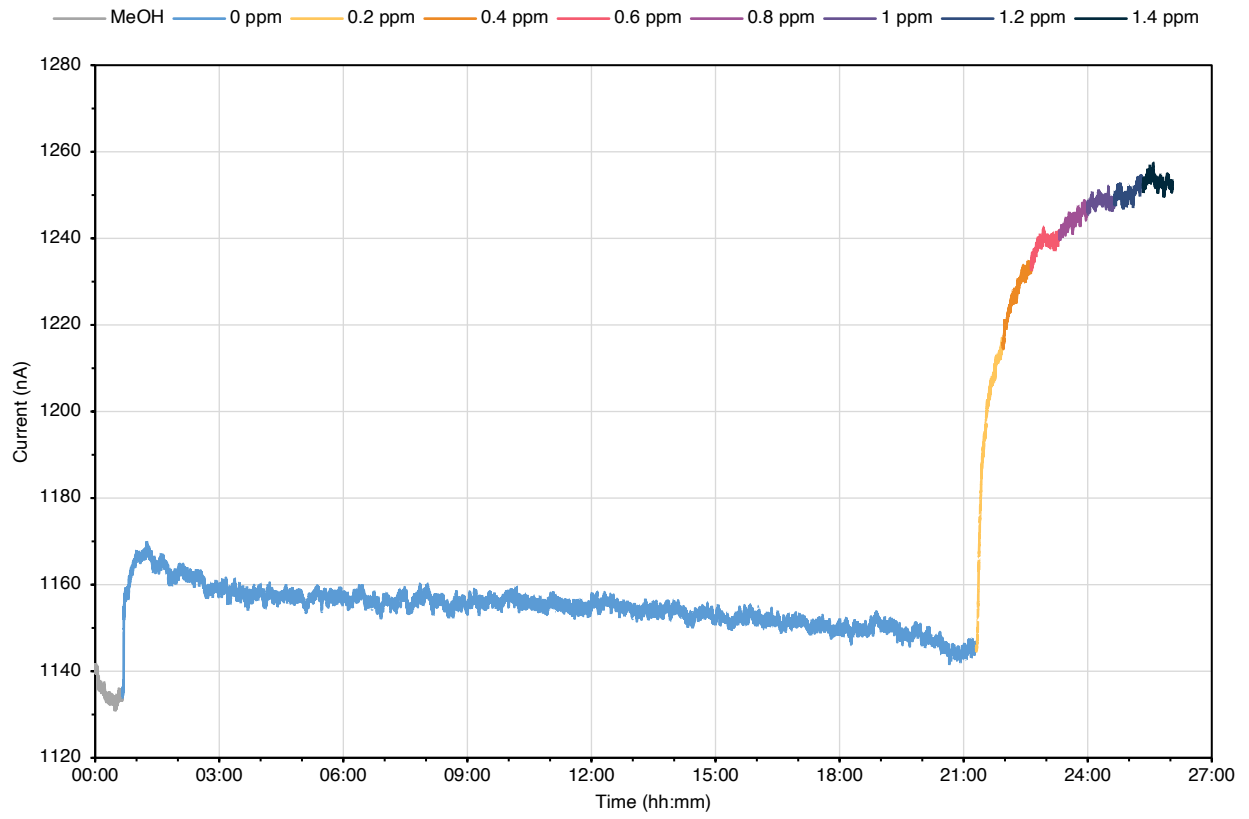
24 nm, 10 mV, doped (1)



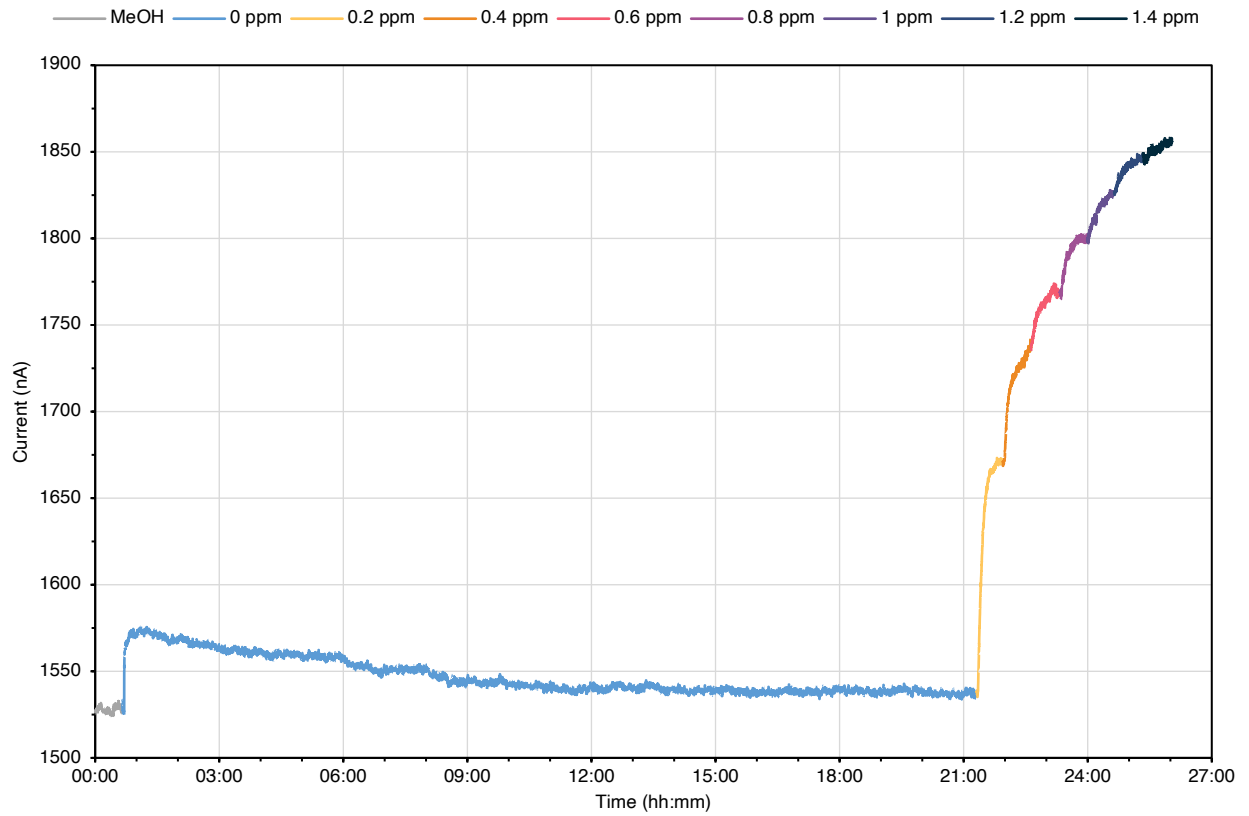
24 nm, 10 mV, doped (2)



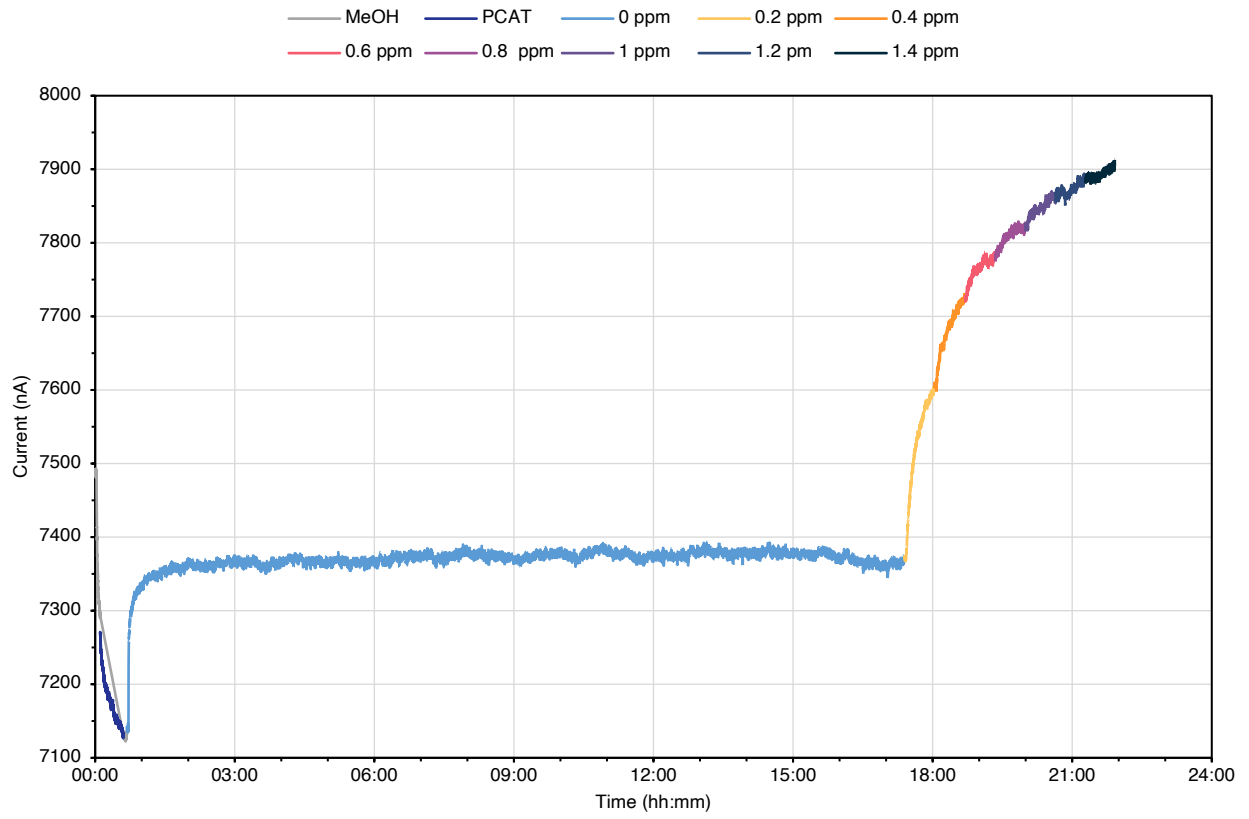
24 nm, 10 mV, blank (1)



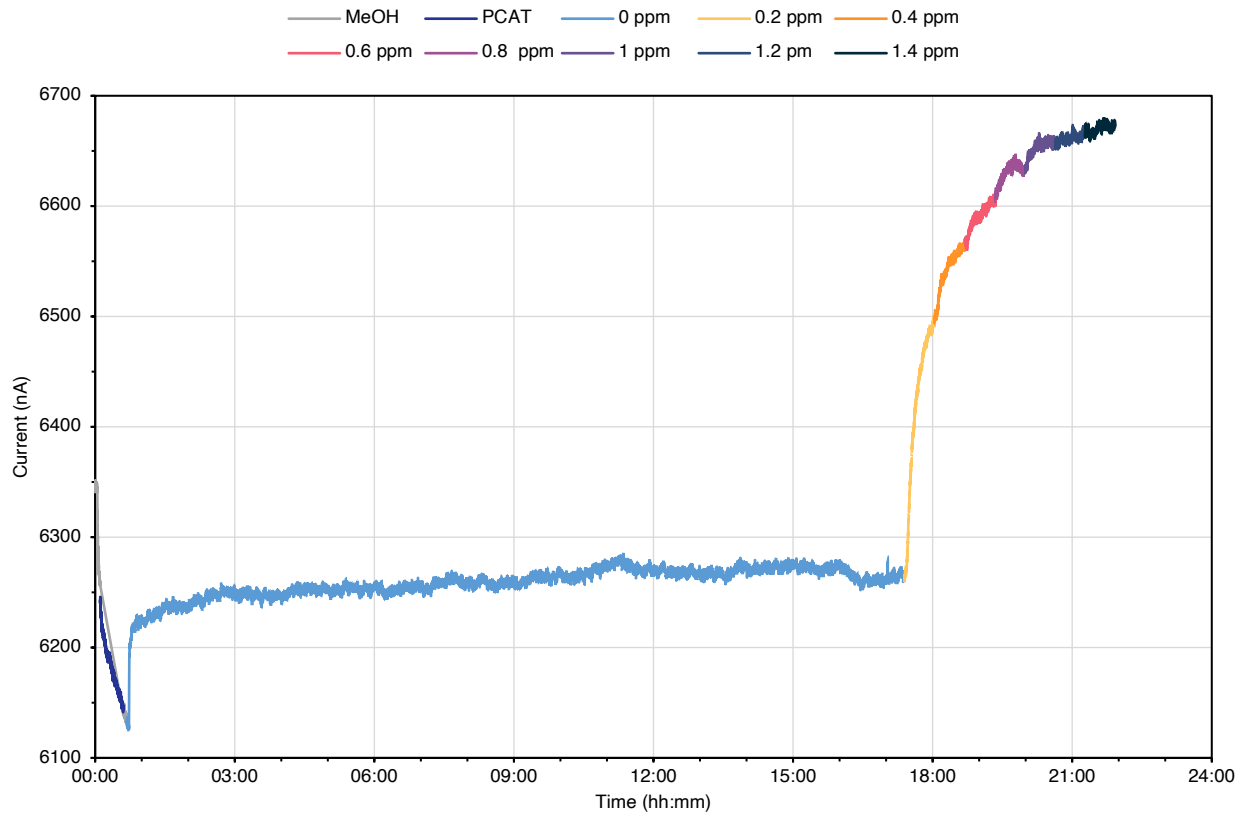
24 nm, 10 mV, blank (2)



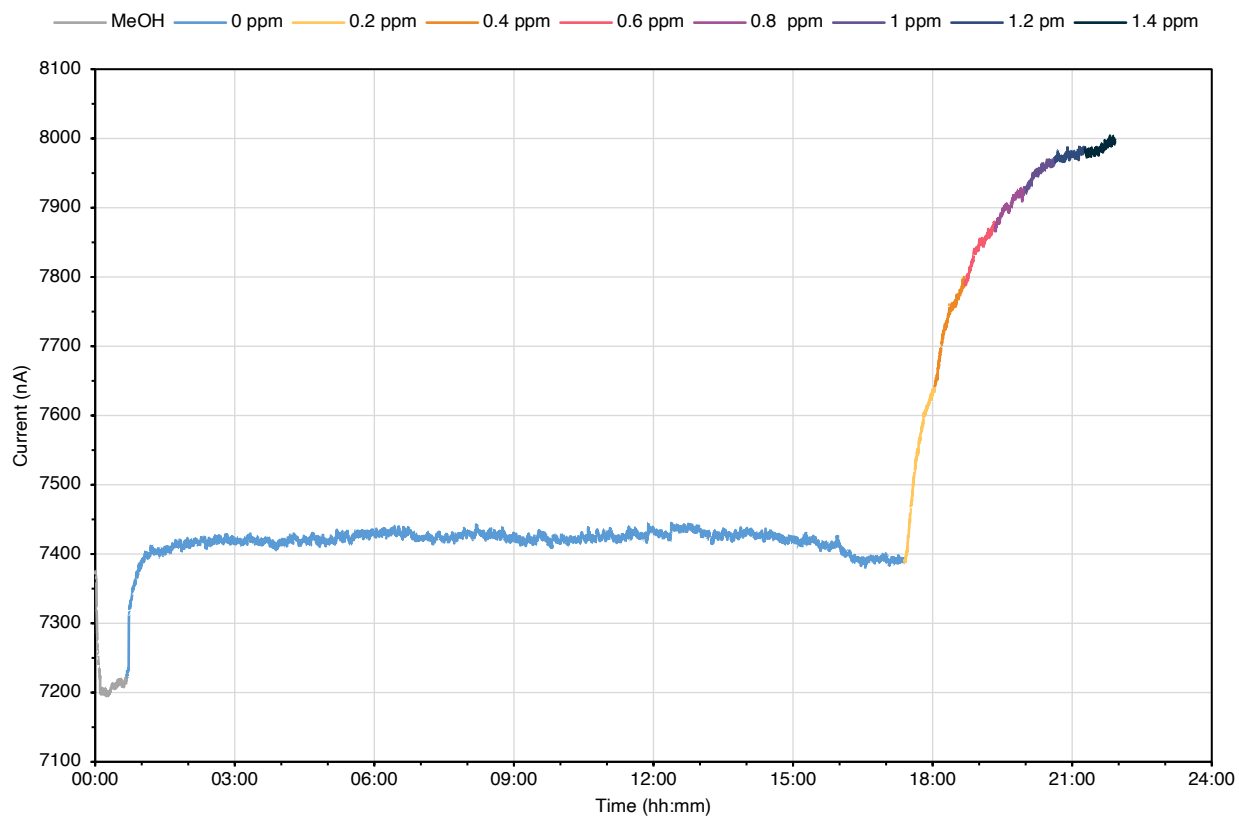
38 nm, 10 mV, doped (1)



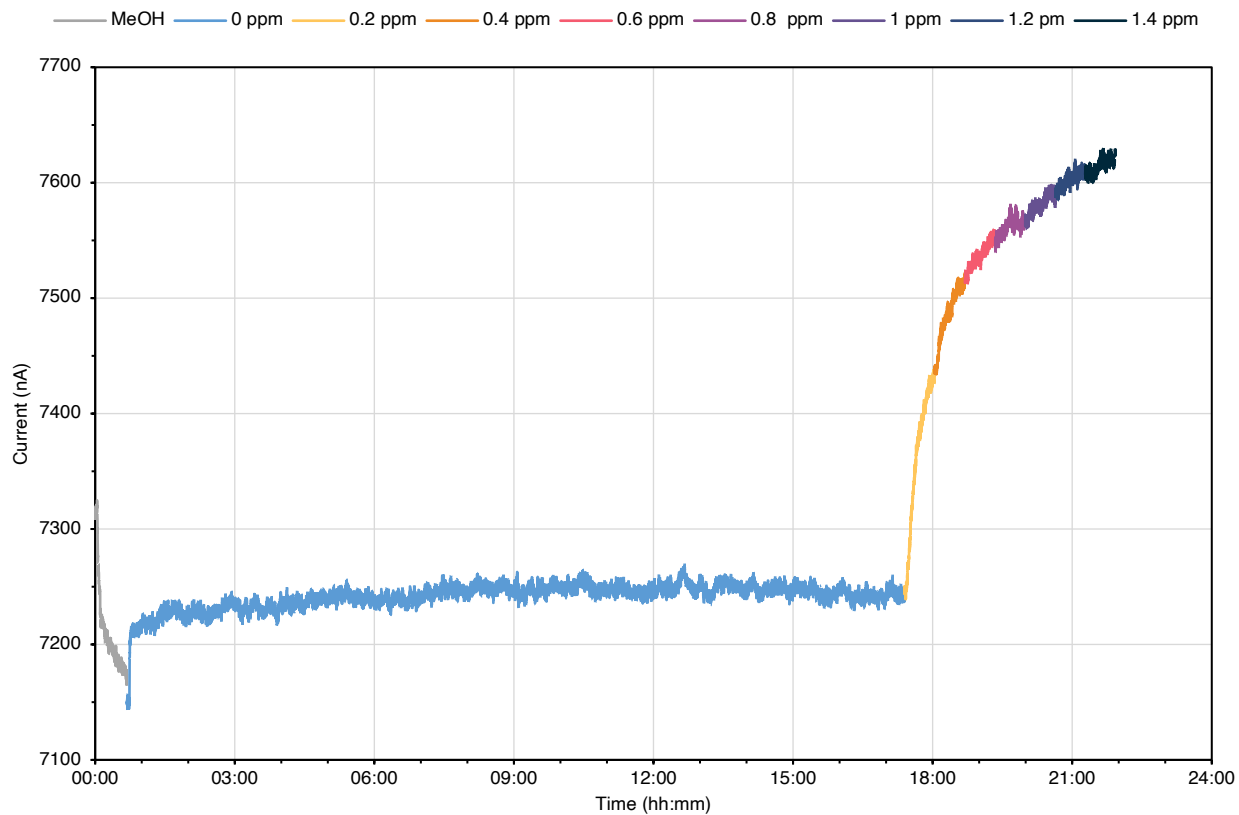
38 nm, 10 mV, doped (2)



38 nm, 10 mV, blank (1)

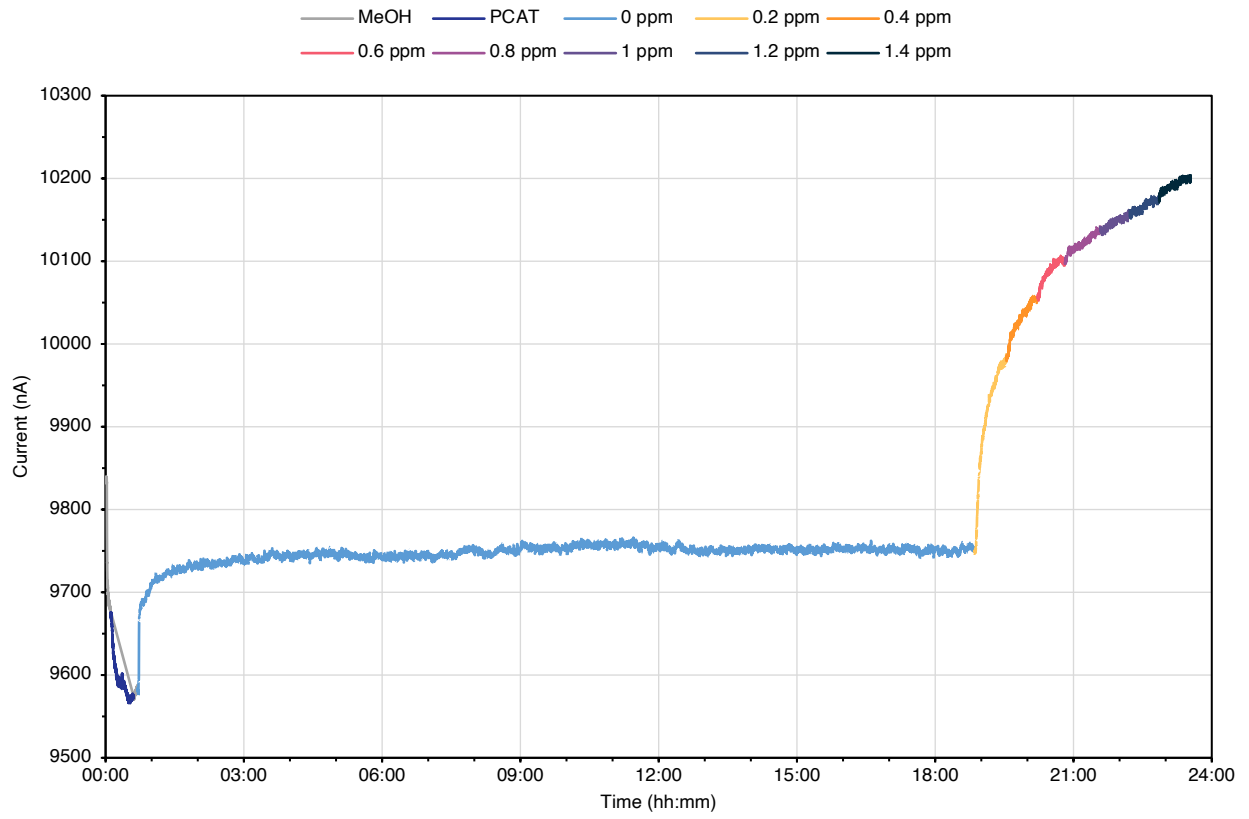


38 nm, 10 mV, blank (2)

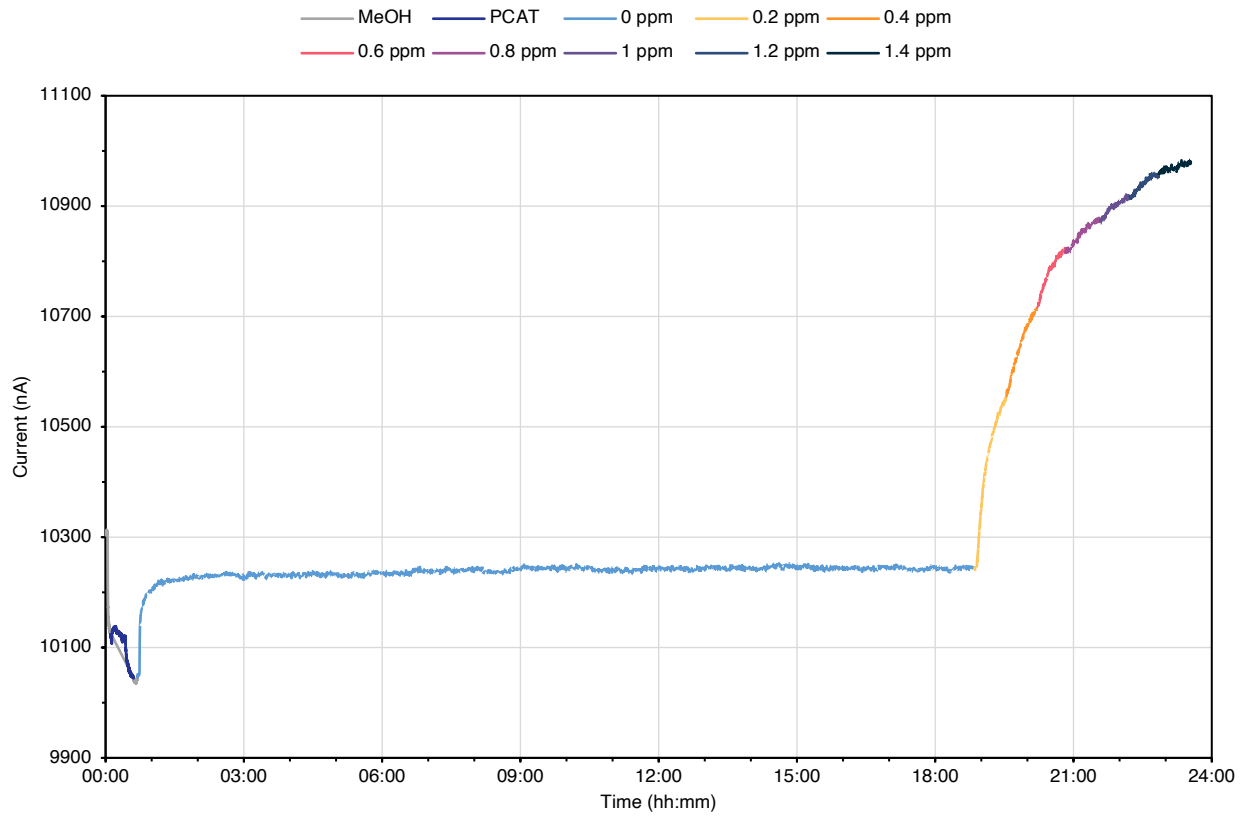




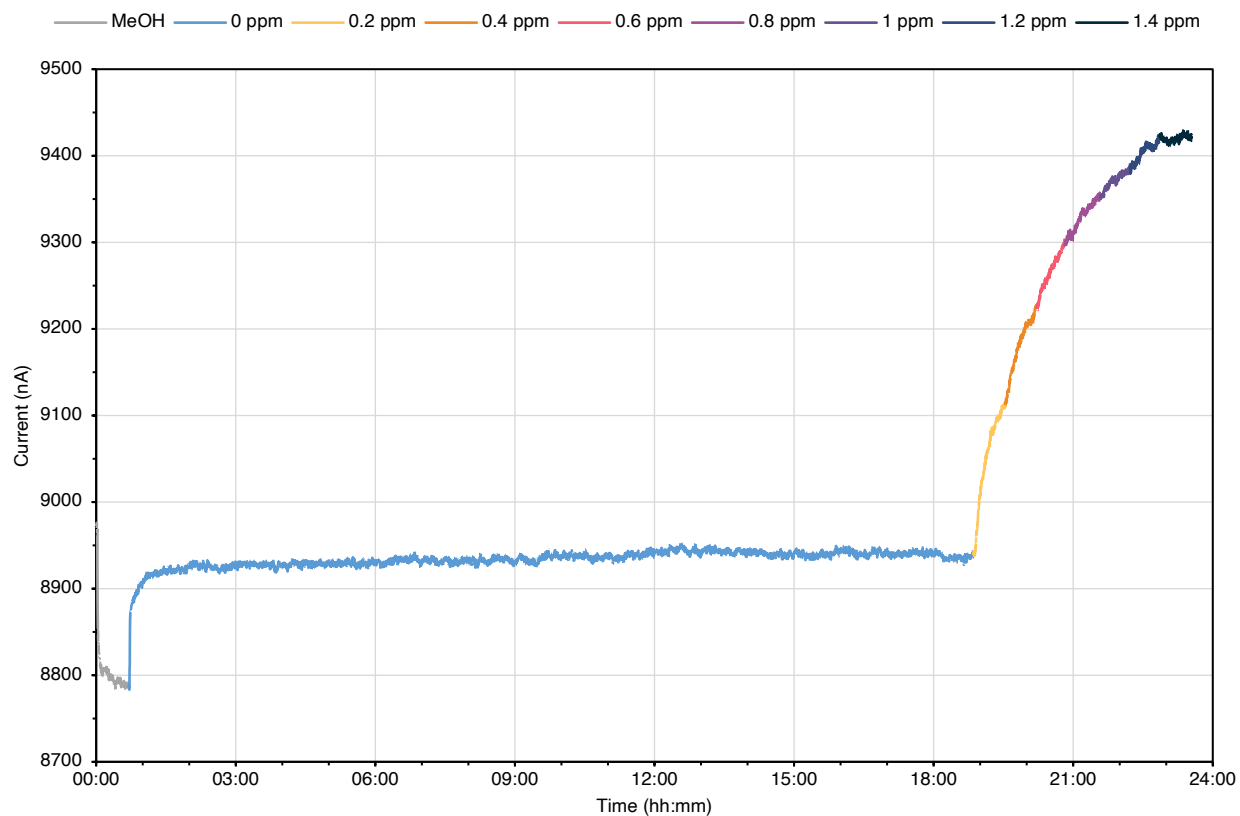
46 nm, 10 mV, doped (1)



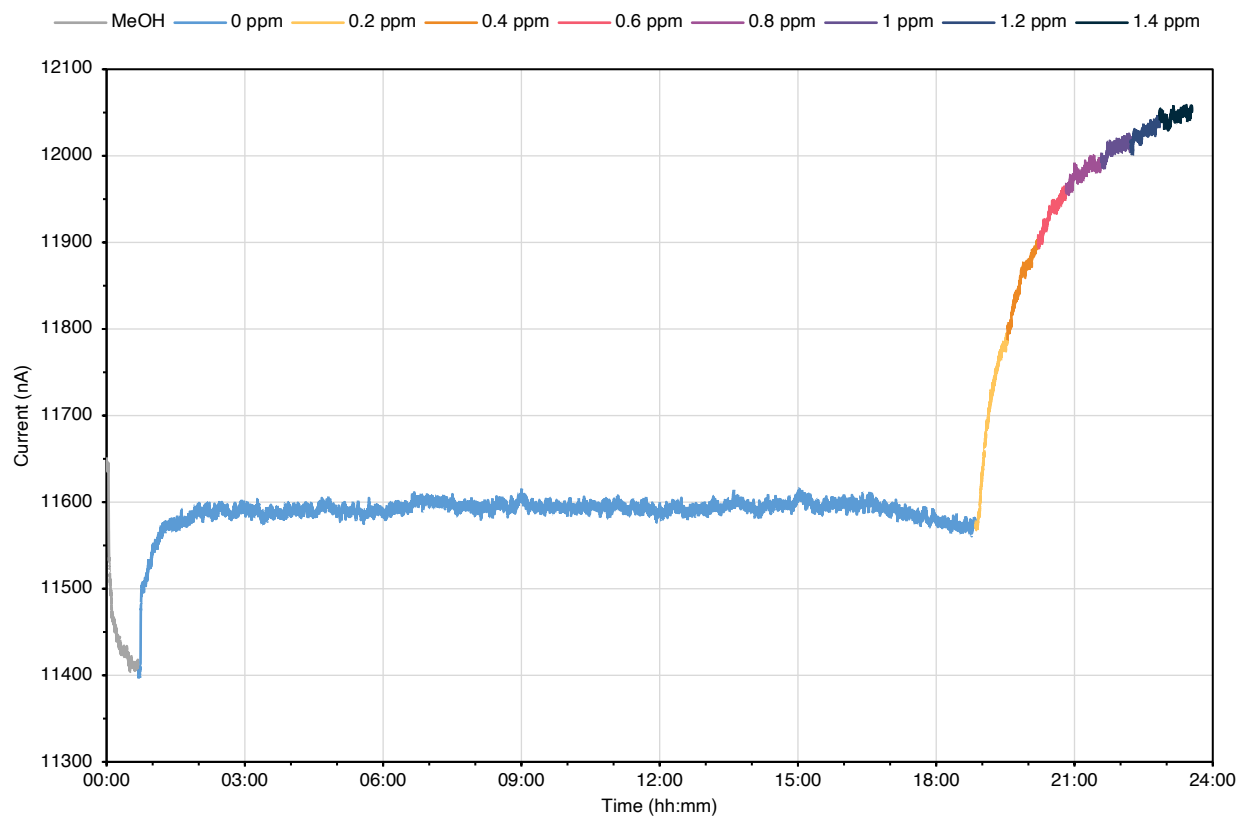
46 nm, 10 mV, doped (2)



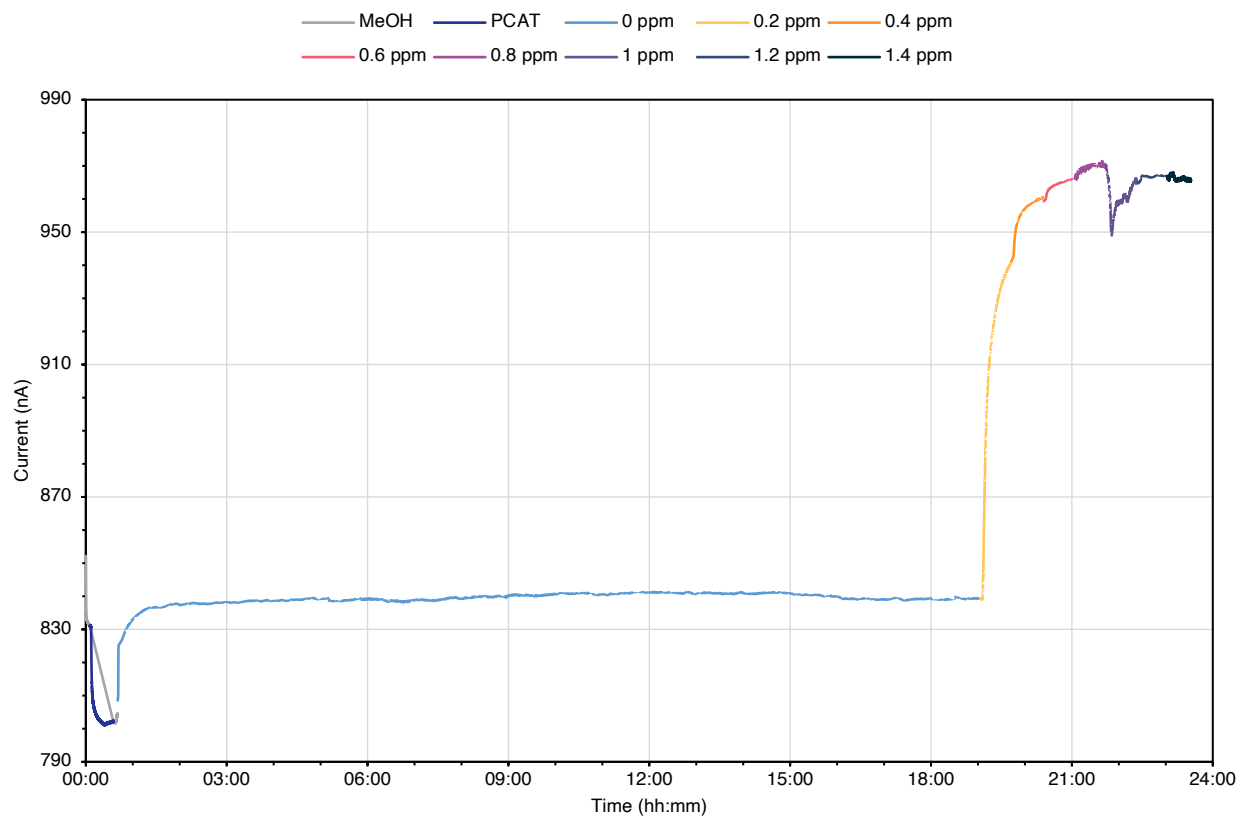
46 nm, 10 mV, blank (1)



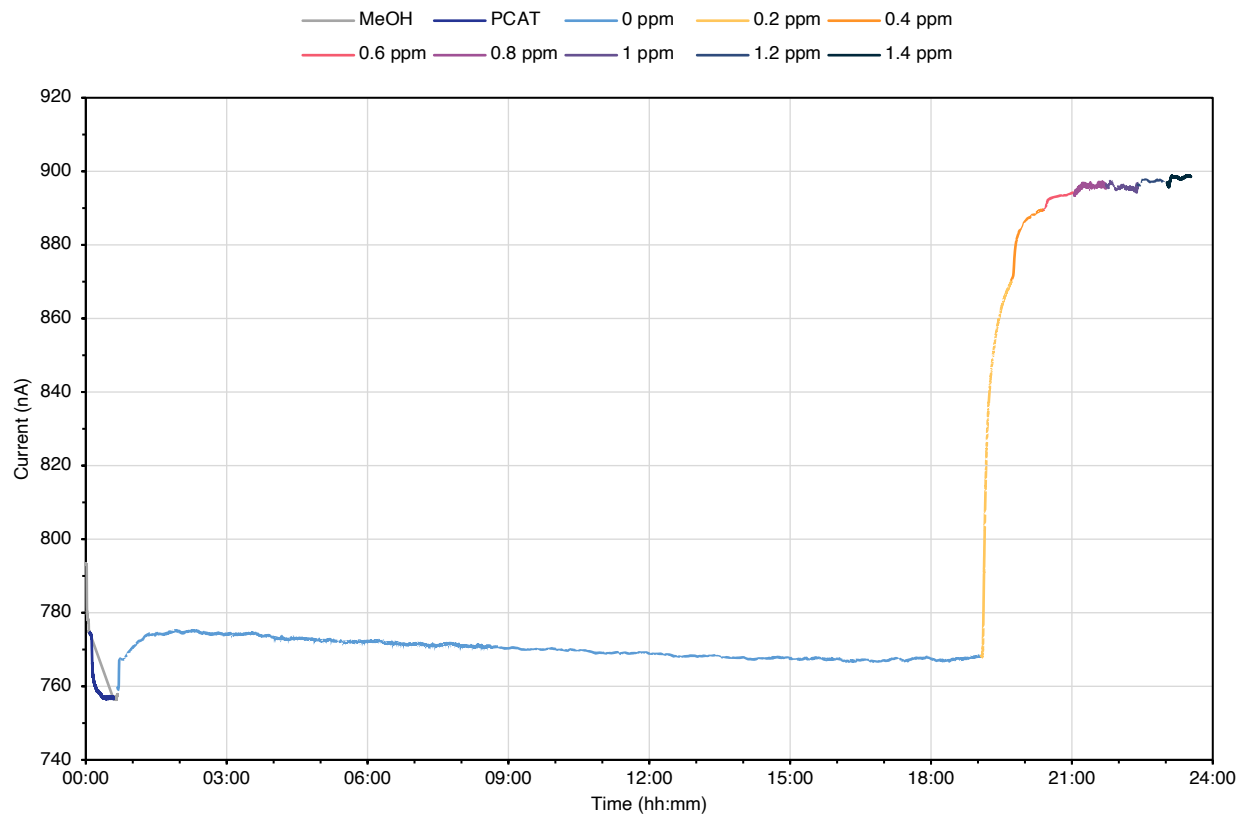
46 nm, 10 mV, blank (2)



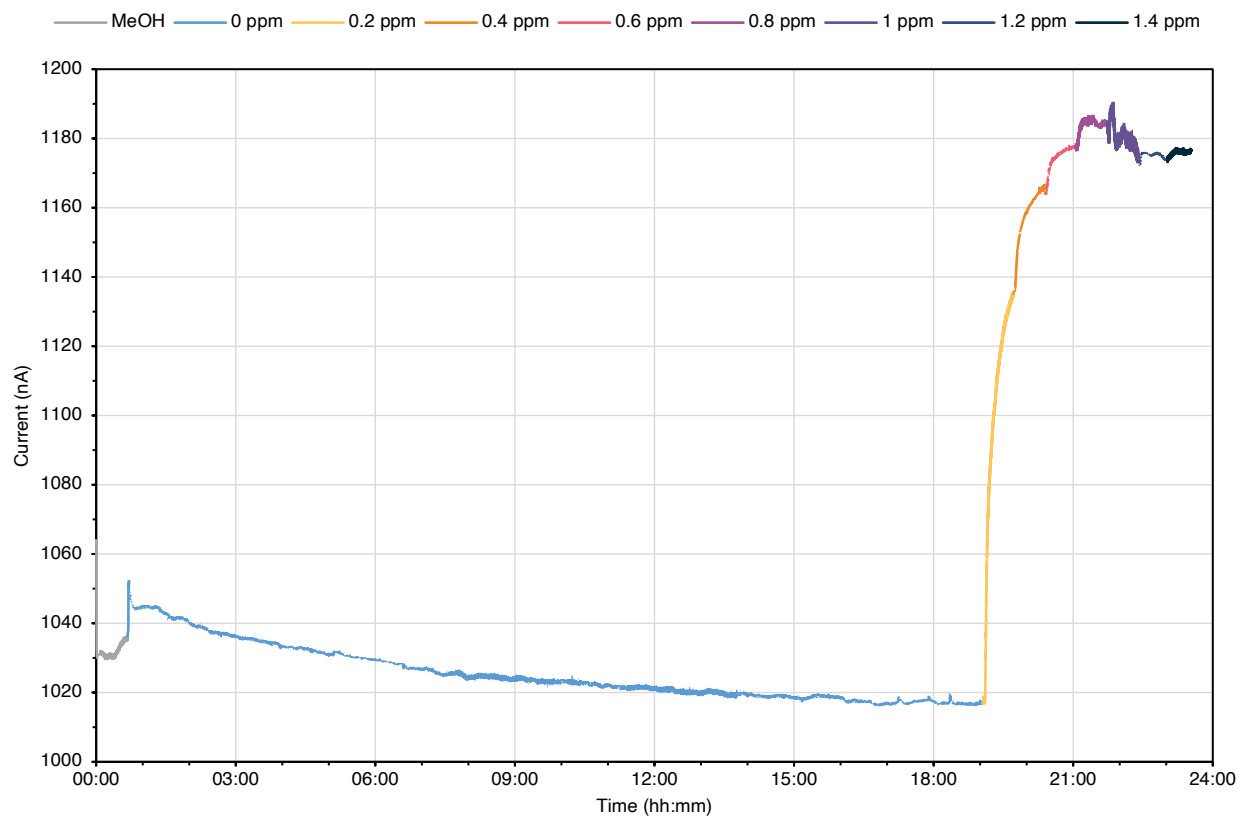
12 nm, 100 mV, doped (1)



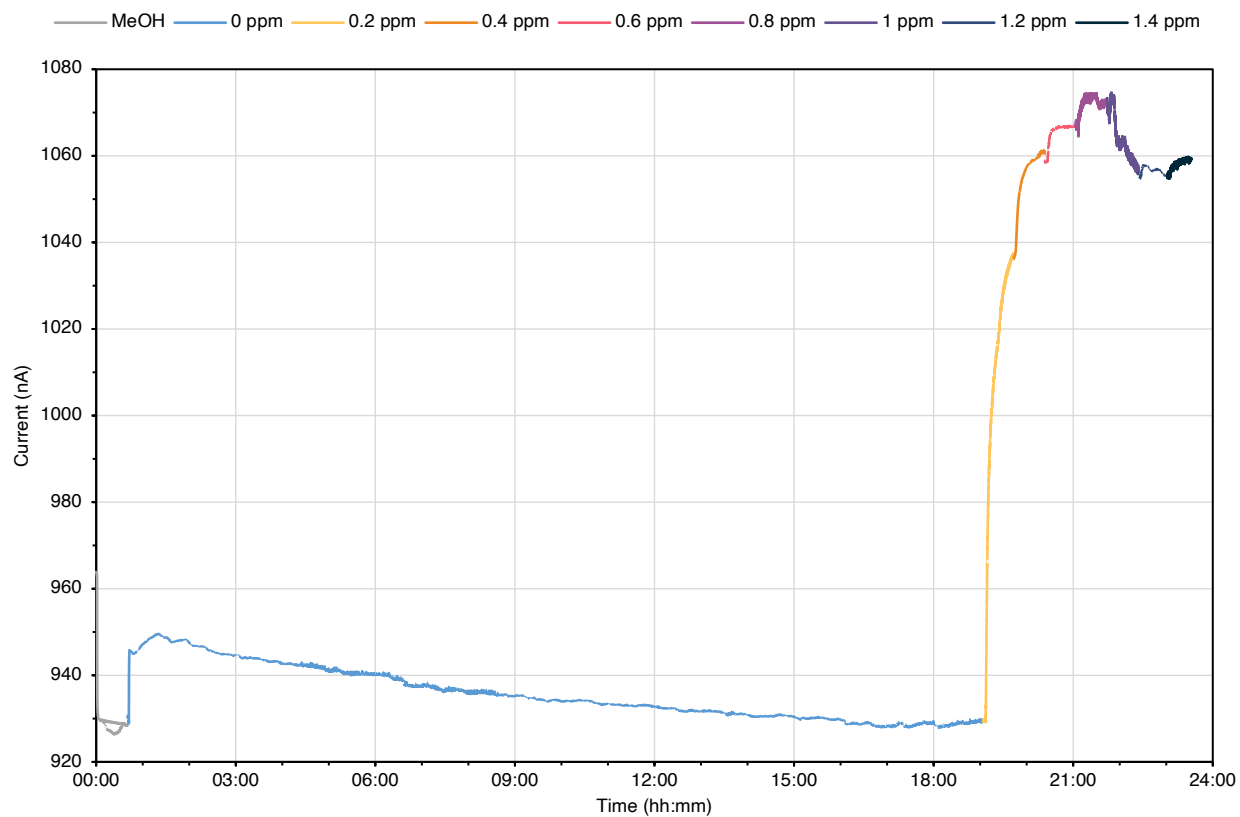
12 nm, 100 mV, doped (2)



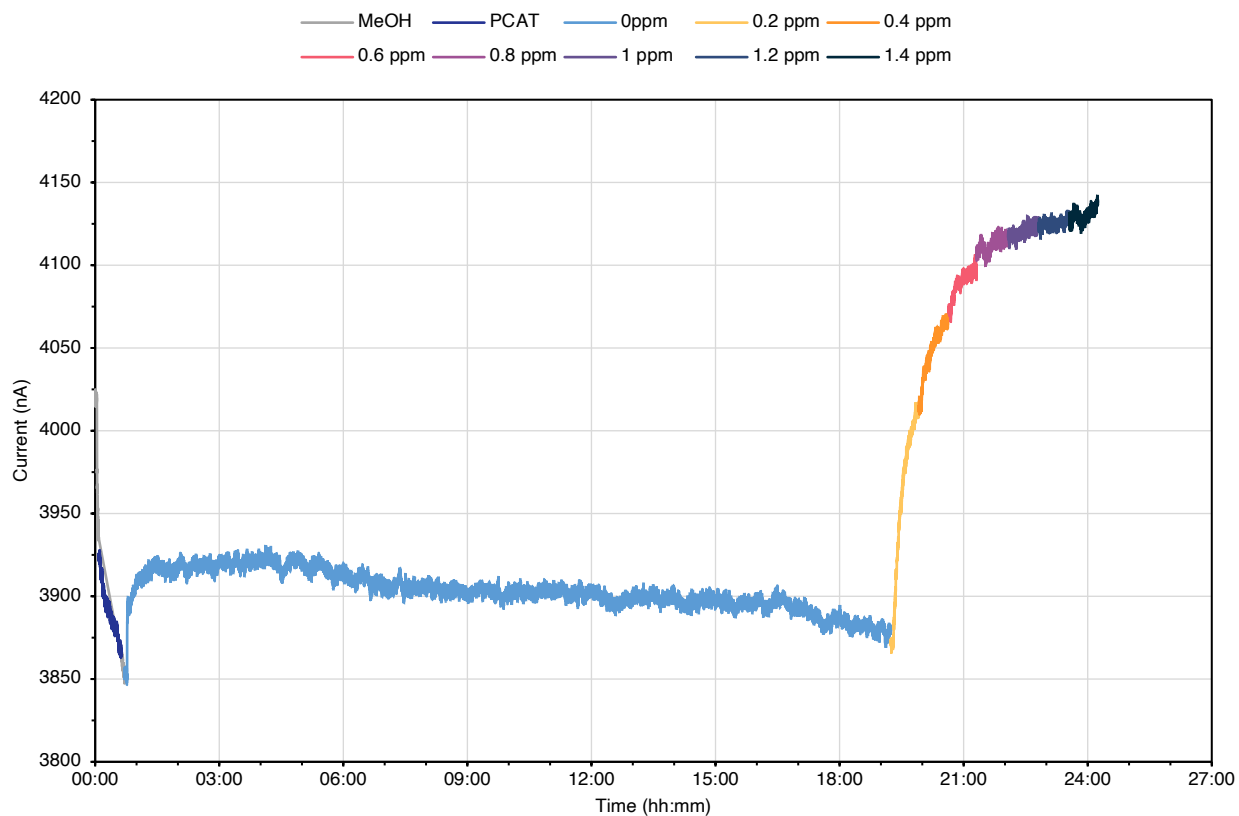
12 nm, 100 mV, blank (1)



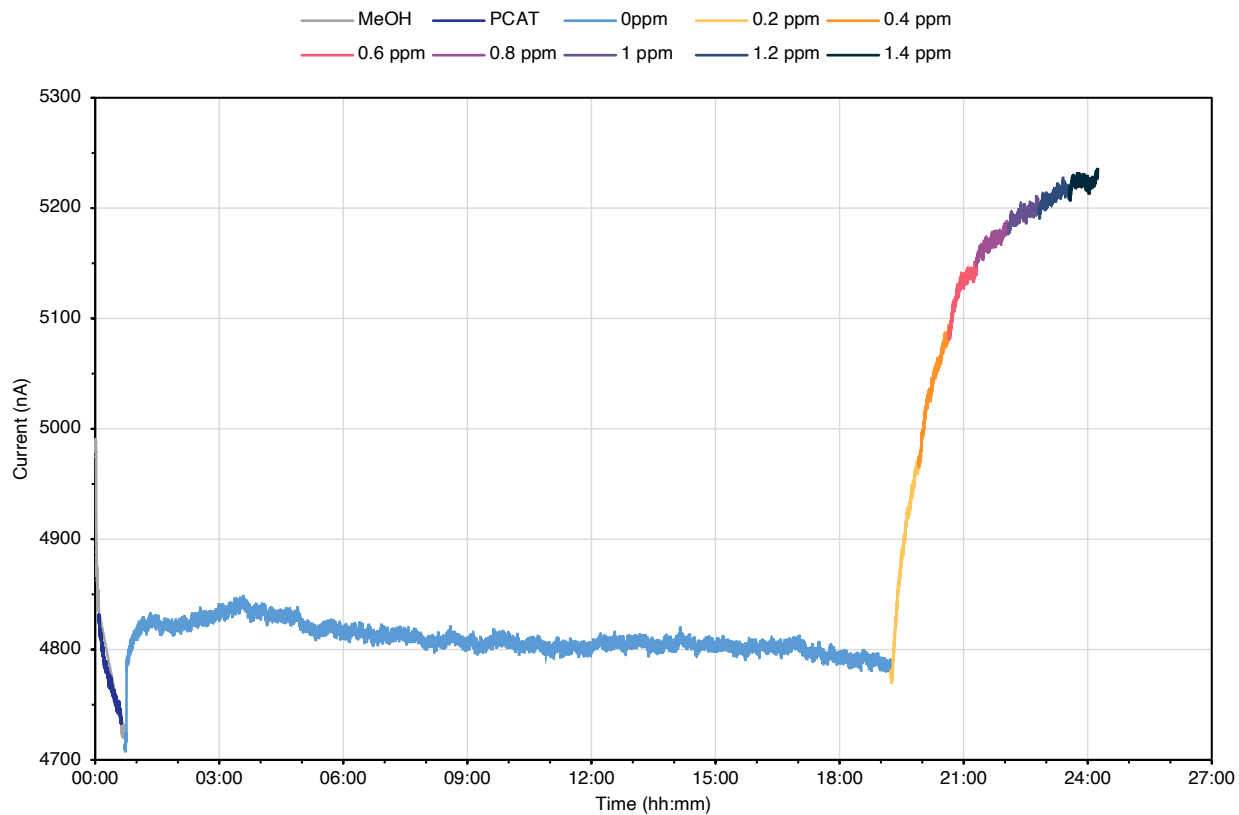
12 nm, 100 mV, blank (2)



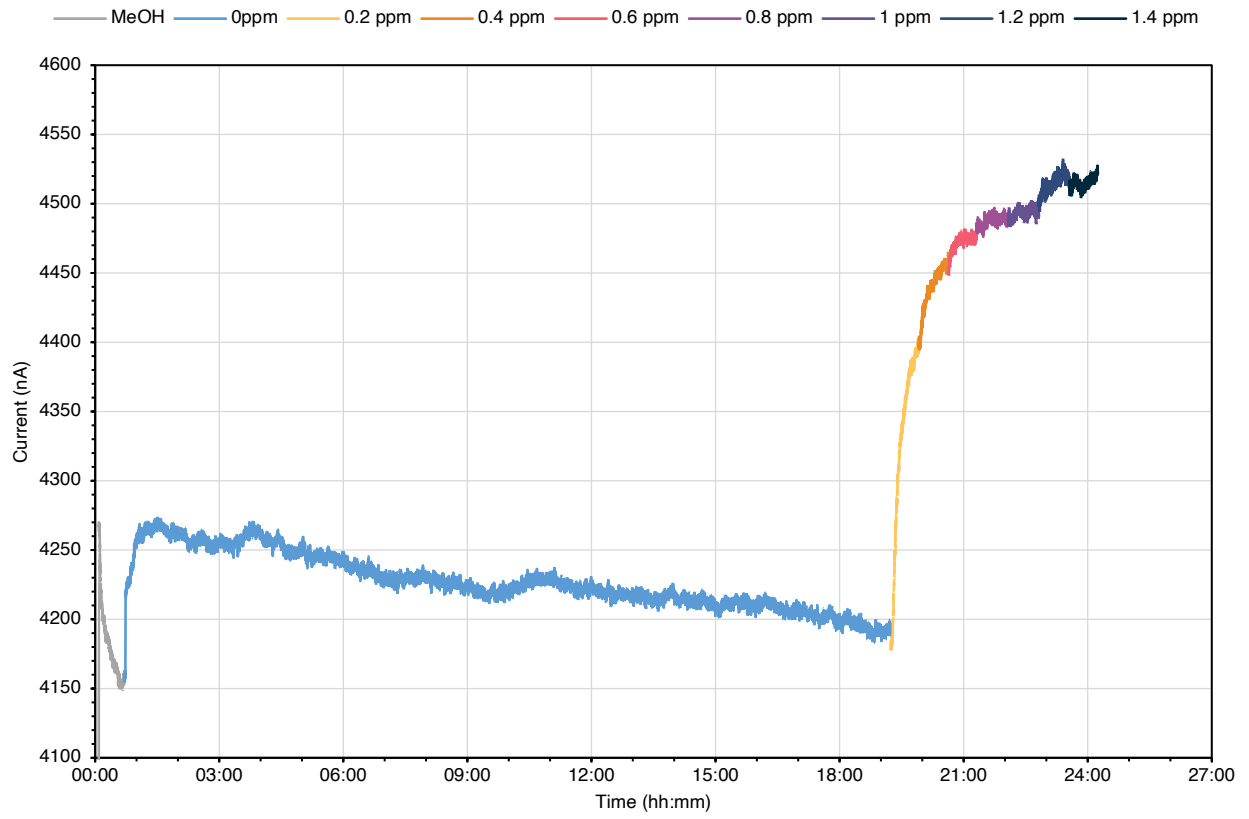
38 nm, 100 mV, doped (1)



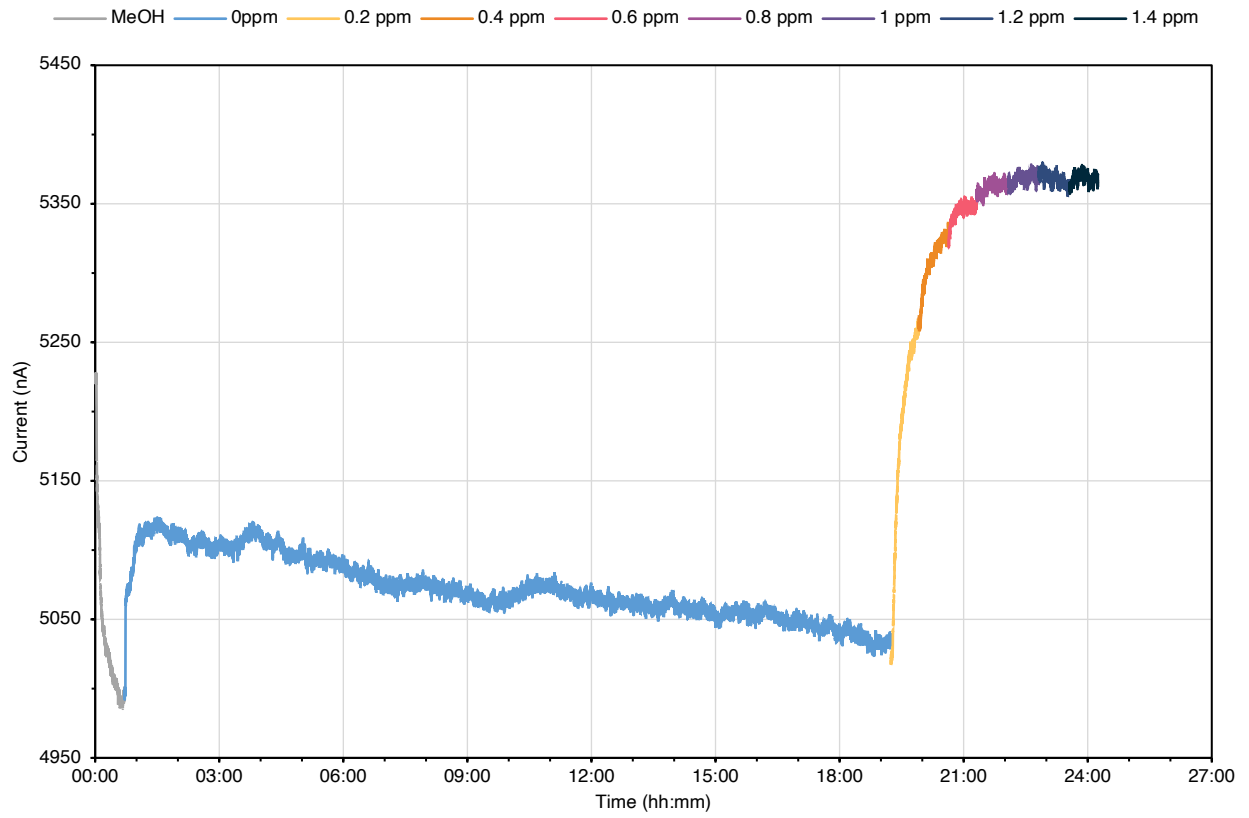
38 nm, 100 mV, doped (2)



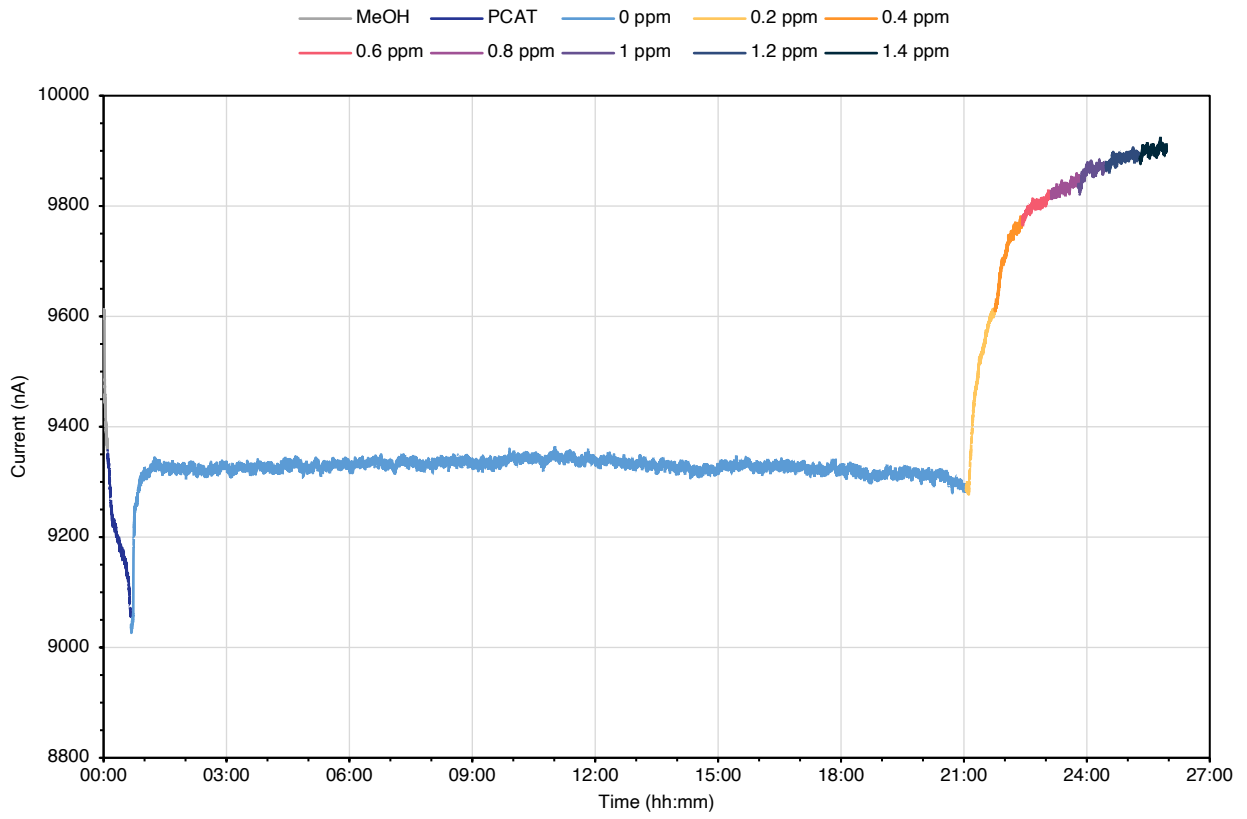
38 nm, 100 mV, blank (1)



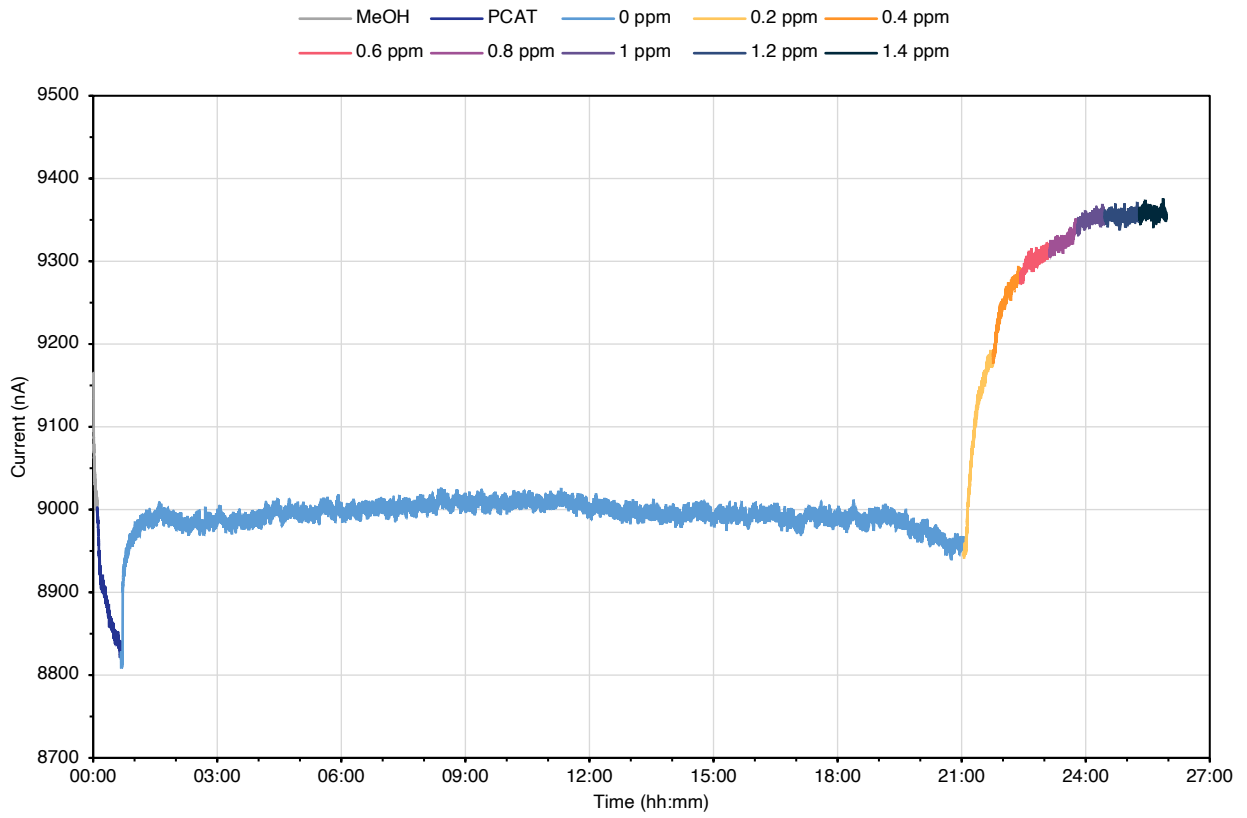
38 nm, 100 mV, blank (2)



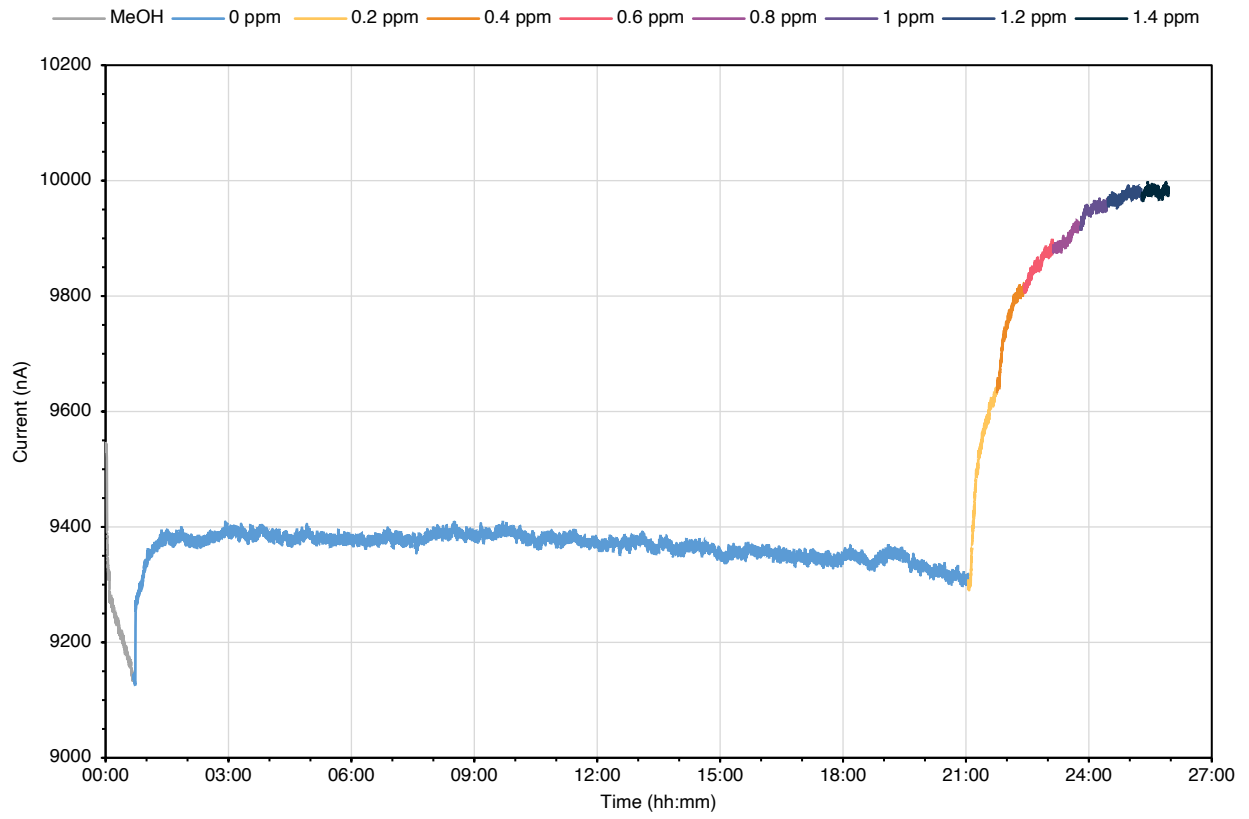
46 nm, 100 mV, doped (1)



46 nm, 100 mV, doped (2)



46 nm, 100 mV, blank (1)



46 nm, 100 mV, blank (2)

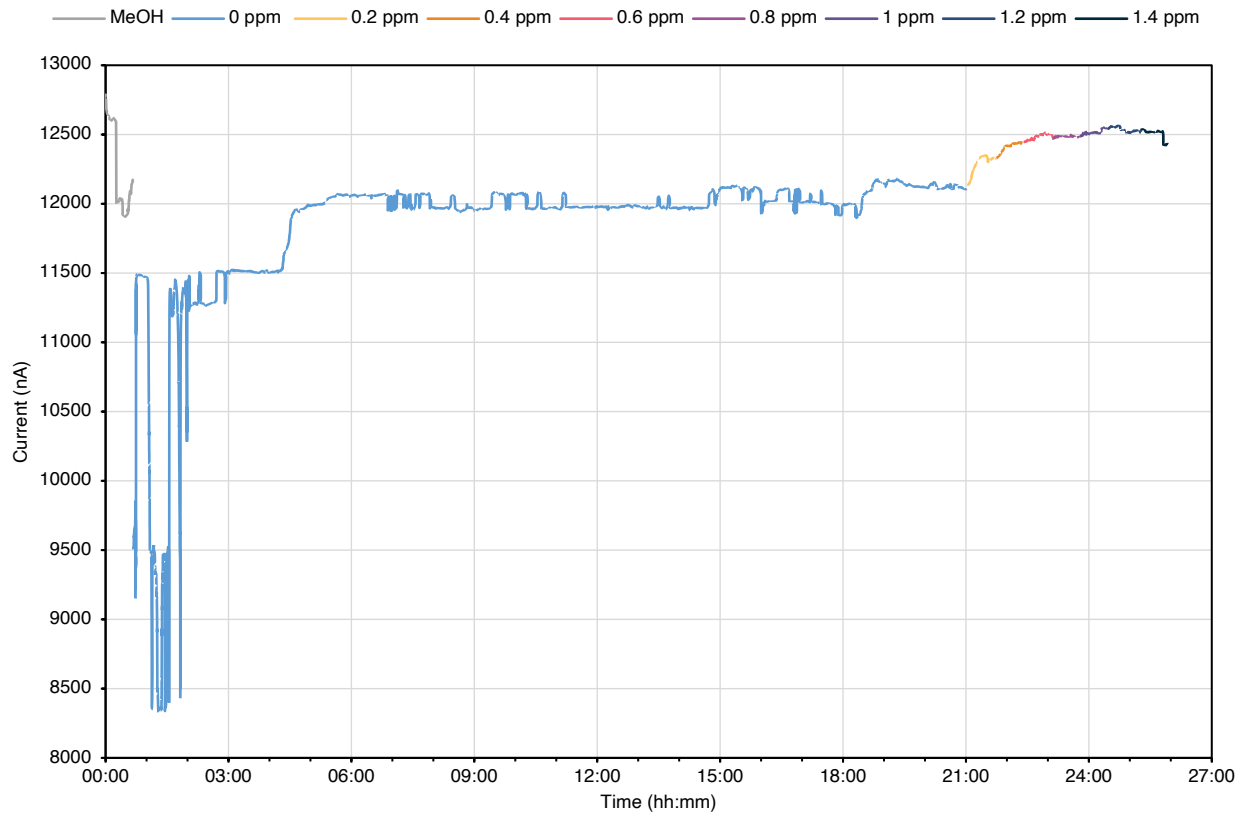




**Table S1.** Equations of the models used to fit the data in **Figure S2**, as well as the curve parameters obtained with each of the sensors.

Langmuir adsorption isotherm:  $y = \frac{ABx}{1+Bx}$

Exponential decay:  $y = i(1 - e^{-jx})$

Freundlich adsorption isotherm:  $y = mx^{1/n}$

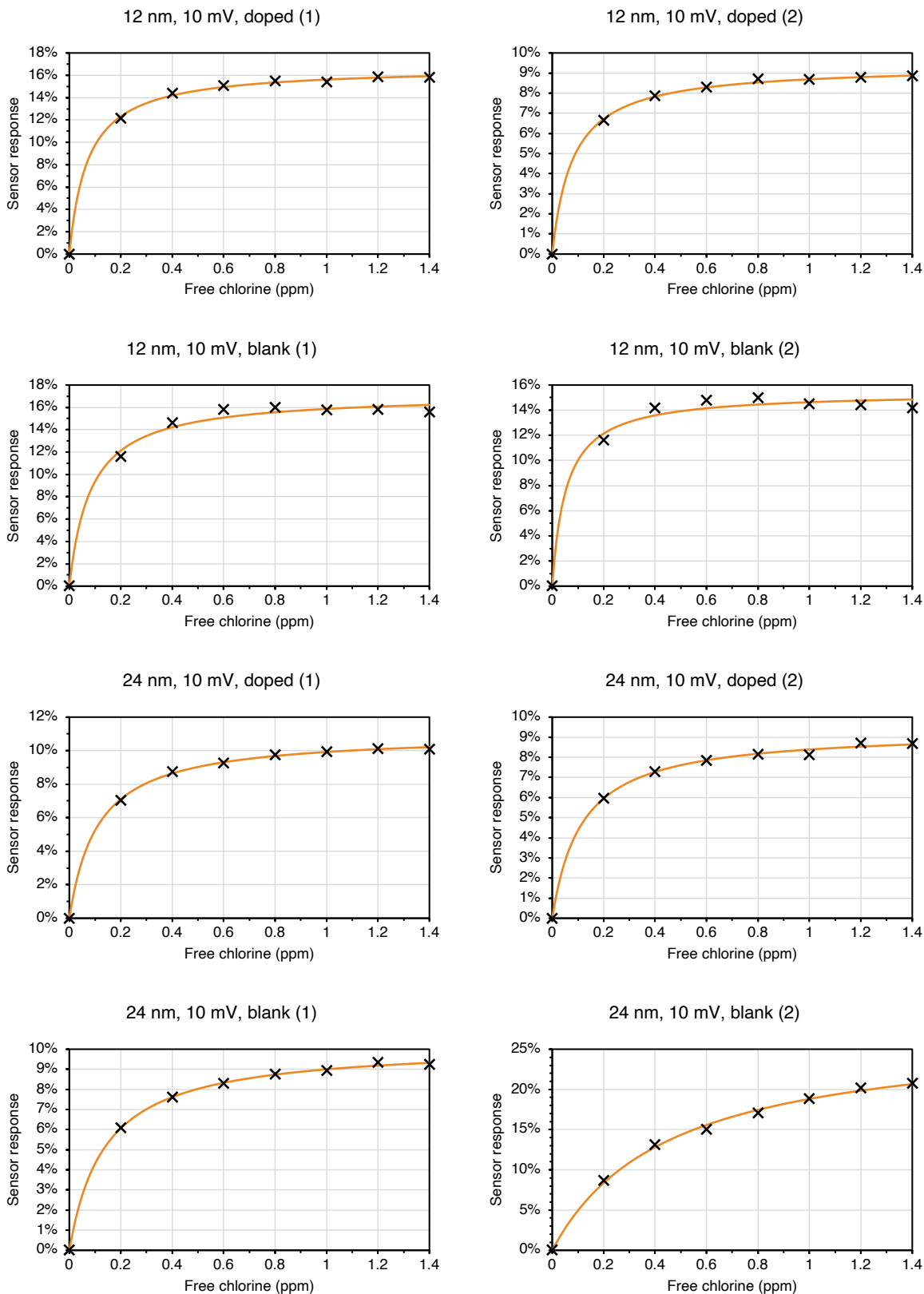
Doped sensors									
Langmuir			Exponential			Freundlich			
A	B	R <sup>2</sup>	i	j	R <sup>2</sup>	m	n	R <sup>2</sup>	
10 mV									
12 nm	0.1678	13.7553	0.9991	0.1556	7.3097	0.9980	0.1516	10.4393	0.9894
12 nm	0.0943	12.2518	0.9994	0.0868	6.8688	0.9967	0.0869	7.3615	0.9948
24 nm	0.1101	9.0850	0.9995	0.0992	5.7888	0.9966	0.0987	5.8172	0.9932
24 nm	0.0934	8.7750	0.9981	0.0838	5.7196	0.9917	0.0835	5.5675	0.9951
38 nm	0.0915	2.6758	0.9993	0.0724	2.6500	0.9963	0.0657	2.6099	0.9919
38 nm	0.0754	4.5298	0.9988	0.0637	3.7066	0.9910	0.0612	3.5431	0.9960
46 nm	0.0535	3.6201	0.9972	0.0441	3.1880	0.9875	0.0414	3.0805	0.9983
46 nm	0.0931	2.4328	0.9998	0.0727	2.4905	0.9981	0.0650	2.4879	0.9911
100 mV									
12 nm	0.1612	17.2411	0.9949	0.1517	7.9730	0.9987	0.1516	10.4396	0.9874
12 nm	0.1783	15.8516	0.9985	0.1669	7.8144	0.9994	0.1671	9.3111	0.9930
38 nm	0.0788	3.9558	0.9991	0.0654	3.4401	0.9981	0.0622	3.2825	0.9879
38 nm	0.1203	2.5774	0.9966	0.0943	2.6263	0.9993	0.0854	2.5631	0.9801
46 nm	0.0770	4.4994	0.9973	0.0648	3.7705	0.9977	0.0623	3.5559	0.9839
46 nm	0.0520	5.0905	0.9945	0.0444	4.0623	0.9989	0.0430	3.9017	0.9770
Blank sensors									
Langmuir			Exponential			Freundlich			
A	B	R <sup>2</sup>	i	j	R <sup>2</sup>	m	n	R <sup>2</sup>	
10 mV									
12 nm	0.1720	11.9299	0.9924	0.1585	6.5844	0.9990	0.1576	7.6494	0.9799
12 nm	0.1544	18.3155	0.9896	0.1461	8.0345	0.9973	0.1455	11.6104	0.9798
24 nm	0.1024	7.2660	0.9994	0.0905	5.0544	0.9937	0.0894	4.8867	0.9945
24 nm	0.2735	2.2057	0.9980	0.2115	2.2973	0.9931	0.1541	0.0000	#DIV/0!
38 nm	0.1084	2.4534	0.9977	0.0846	2.5263	0.9996	0.0759	2.5028	0.9829
38 nm	0.0609	3.8946	0.9980	0.0505	3.4058	0.9930	0.0479	3.2239	0.9916
46 nm	0.0778	1.7693	0.9984	0.0579	2.0198	0.9996	0.0489	2.1297	0.9868
46 nm	0.0515	2.8837	0.9993	0.0411	2.7989	0.9979	0.0377	2.7218	0.9891

---

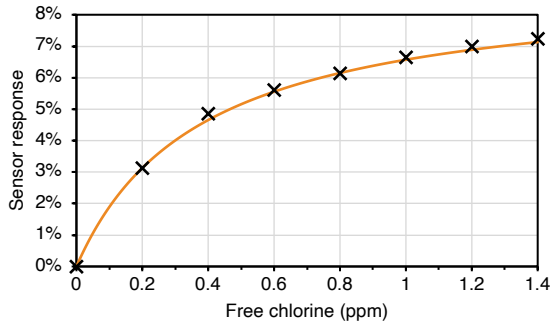
100 mV									
12 nm	0.1715	12.1452	0.9877	0.1583	6.6069	0.9960	0.1572	7.8573	0.9741
12 nm	0.1495	23.0048	0.9741	0.1432	8.6211	0.9845	0.1422	15.6823	0.9643
38 nm	0.0852	6.5103	0.9973	0.0745	4.7763	0.9894	0.0734	4.4752	0.9945
38 nm	0.0729	8.6910	0.9962	0.0656	5.5911	0.9991	0.0649	5.7617	0.9841
46 nm	0.0881	3.6779	0.9971	0.0725	3.3051	0.9991	0.0684	3.1457	0.9814
46 nm	0.0379	6.2814	0.9307	0.0332	4.5225	0.9495	0.0323	4.7866	0.8995

---

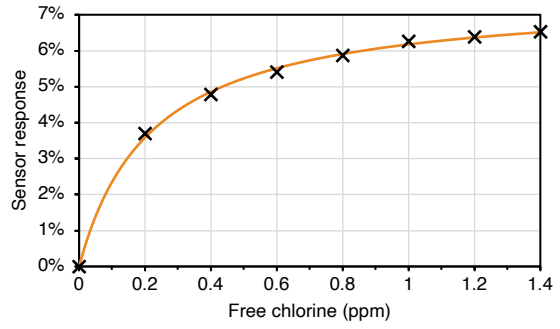
**Figure S3.** Calibration curves obtained with the raw data in **Figure S2**, fitted to a Langmuir adsorption isotherm using the curve parameters in **Table S1**.



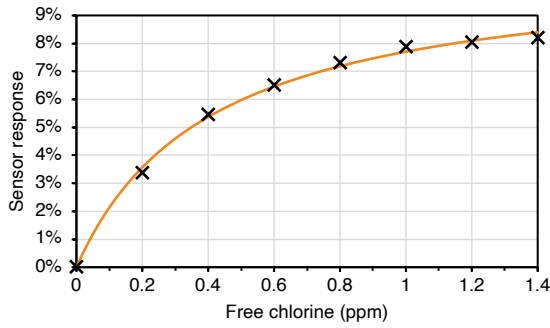
38 nm, 10 mV, doped (1)



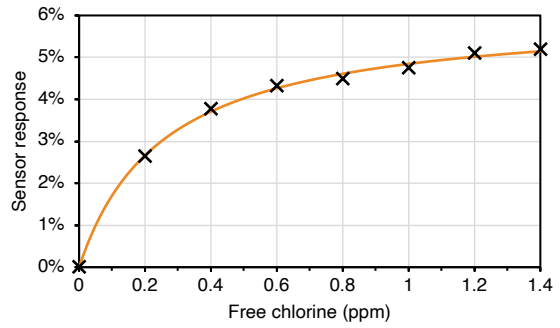
38 nm, 10 mV, doped (2)



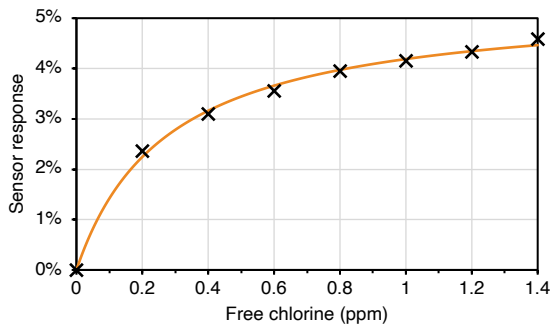
38 nm, 10 mV, blank (1)



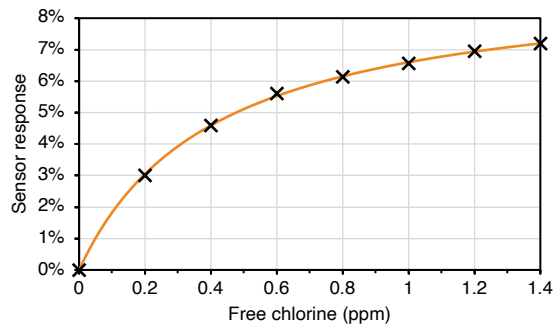
38 nm, 10 mV, blank (2)



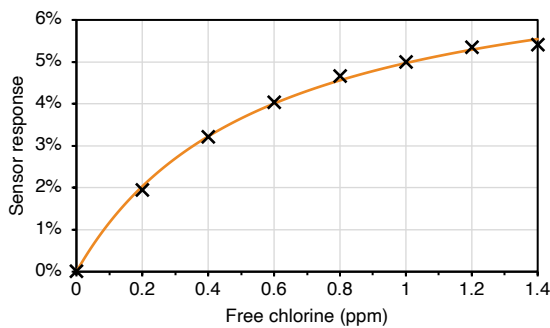
46 nm, 10 mV, doped (1)



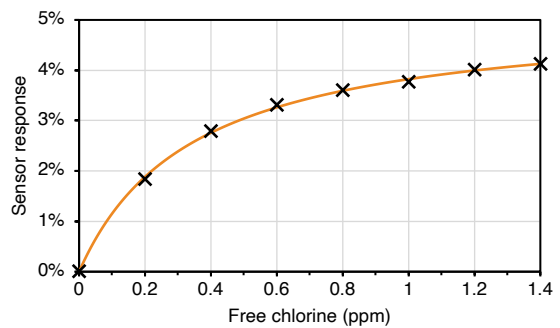
46 nm, 10 mV, doped (2)



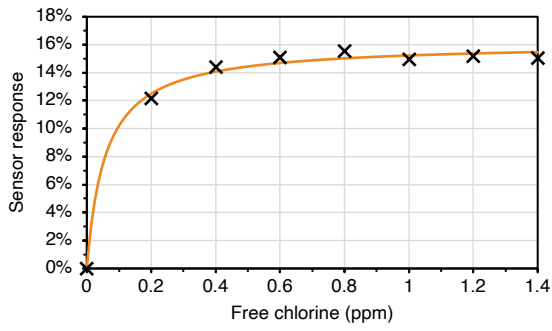
46 nm, 10 mV, blank (1)



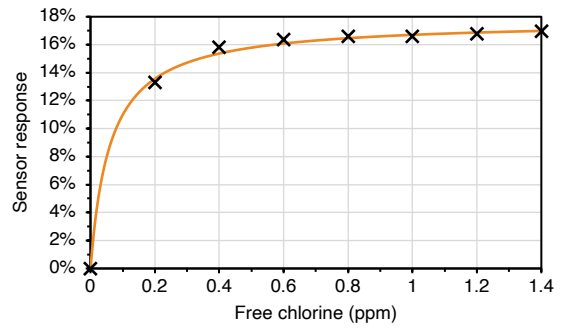
46 nm, 10 mV, blank (2)



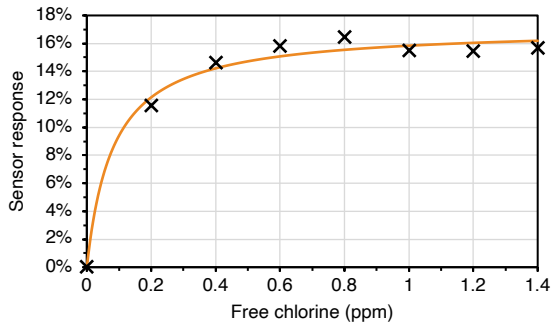
12 nm, 100 mV, doped (1)



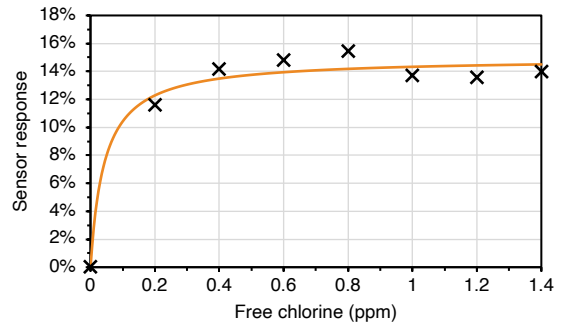
12 nm, 100 mV, doped (2)



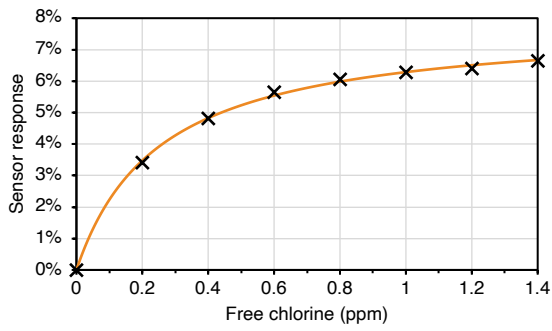
12 nm, 100 mV, blank (1)



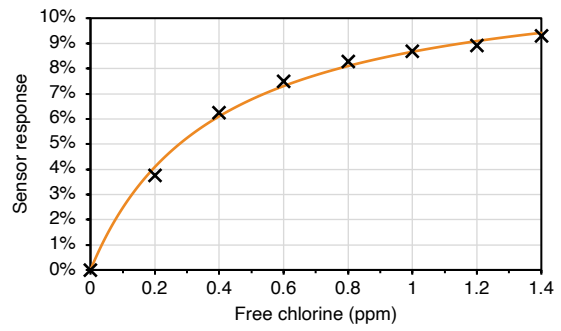
12 nm, 100 mV, blank (2)



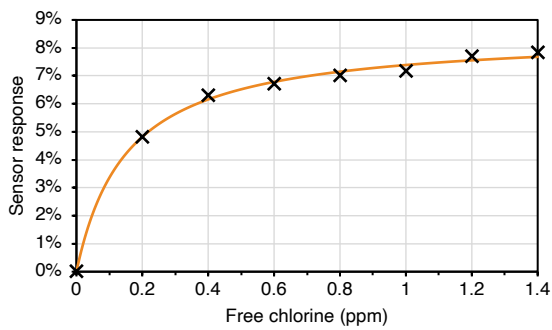
38 nm, 100 mV, doped (1)



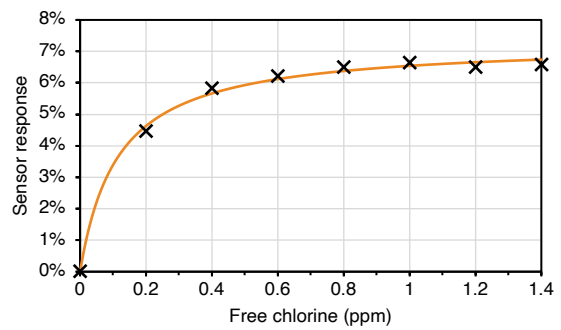
38 nm, 100 mV, doped (2)



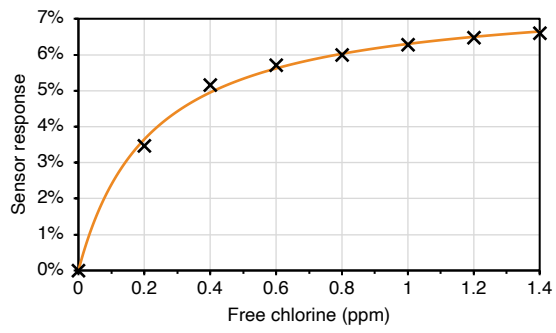
38 nm, 100 mV, blank (1)



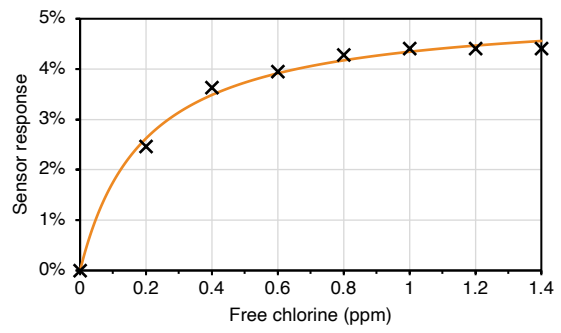
38 nm, 100 mV, blank (2)



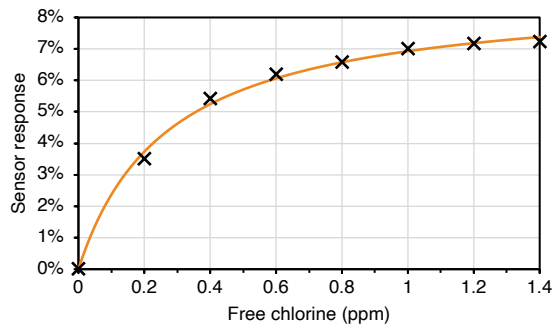
46 nm, 100 mV, doped (1)



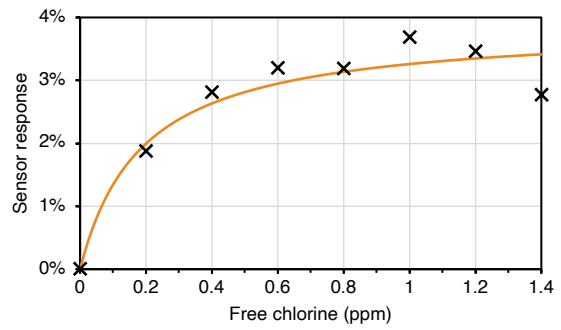
46 nm, 100 mV, doped (2)



46 nm, 100 mV, blank (1)



46 nm, 100 mV, blank (2)



**Equation S1.** Derivation showing that  $1/B$  is proportional to the saturation concentration (SC). When exposed to the saturation concentration, the sensor response ( $y$ ) should be equal to the maximum response ( $A$ ). However, if the sensors are exposed to 95% of the saturation concentration, the sensor response should be 95% of the maximum response. If we rearrange the equation, we get an expression that shows that the saturation concentration is proportional to  $1/B$ .

$$y = \frac{ABx}{1 + Bx} \rightarrow x = \frac{y/A}{1 - y/A} \cdot \frac{1}{B} \rightarrow SC_{95\%} = \frac{0.95}{1 - 0.95} \cdot \frac{1}{B} \rightarrow SC \propto \frac{1}{B}$$

**Figure S4.** Replicates of the low range detection data (calibration curves and raw data from the lowest concentration).

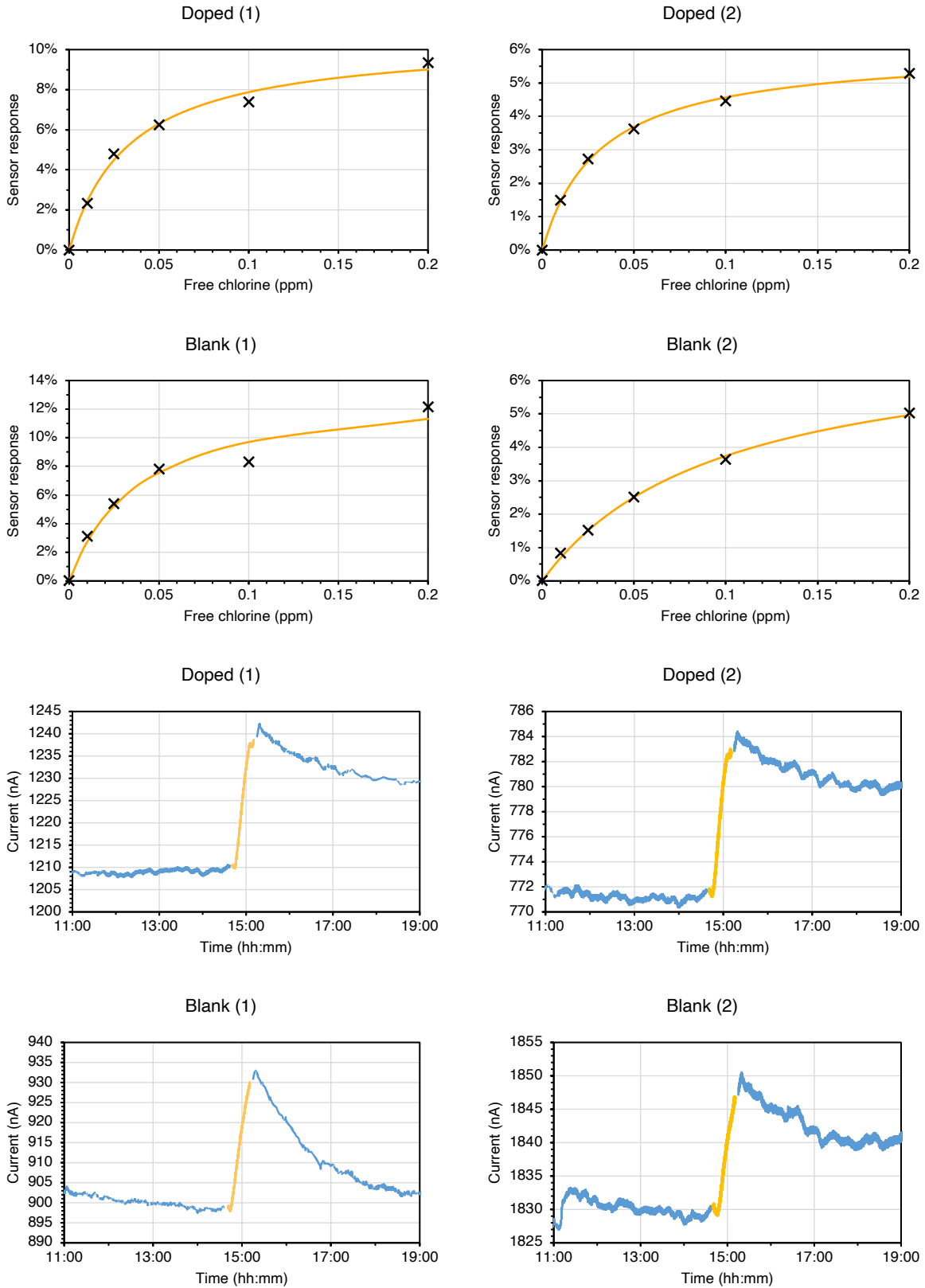
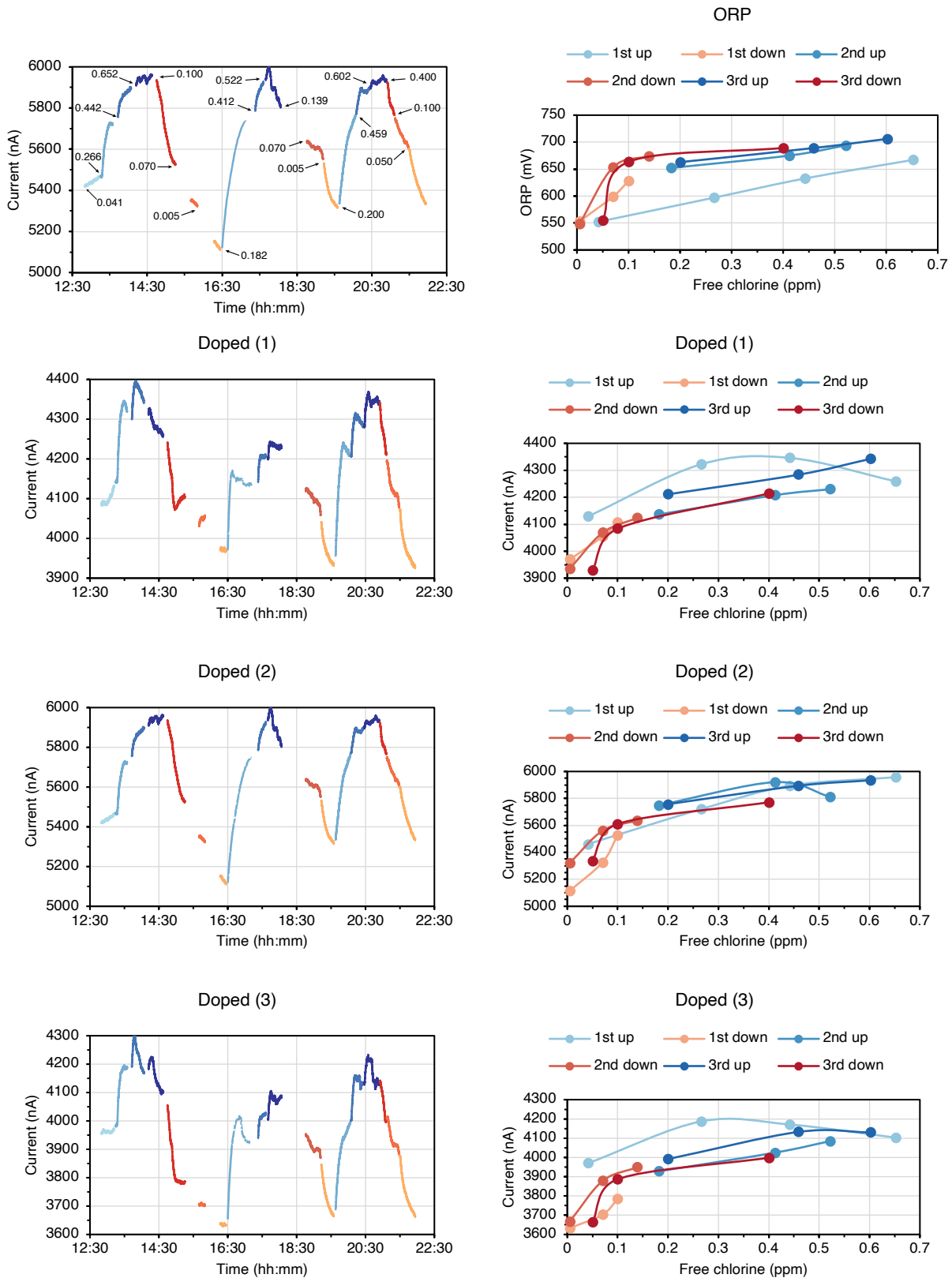




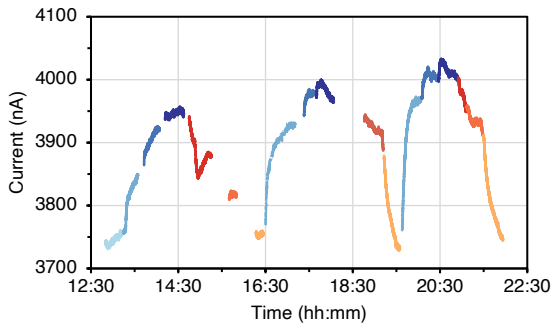
**Table S2.** Curve parameters from the Langmuir adsorption isotherms used to fit the low range detection data shown in **Figure S4**.

	A	B	R <sup>2</sup>
Doped (1)	0.1052	29.8152	0.9922
Doped (2)	0.0601	31.8057	0.9985
Blank (1)	0.1358	25.0066	0.9687
Blank (2)	0.0738	10.2781	0.9978

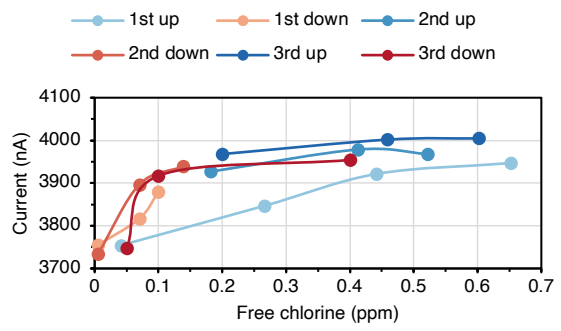
**Figure S5.** Replicates of the detection of free chlorine concentration fluctuations (raw and processed data). The first graph (top left) uses arrows to display where a new free chlorine concentration was introduced and what the concentration was (measured with the DPD method, AquaMate). The second graph (top right) shows the ORP values for each of those concentrations.



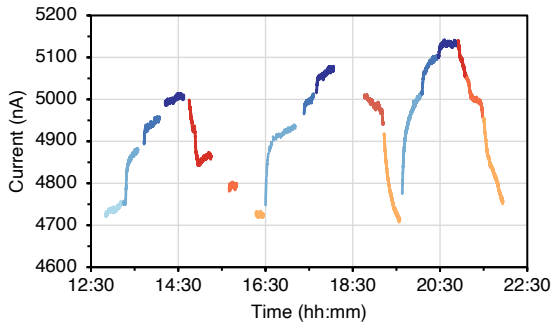
Blank (1)



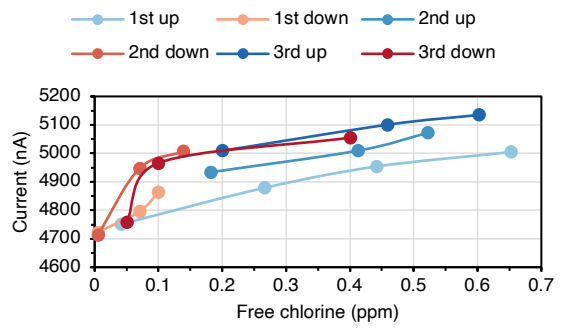
Blank (1)



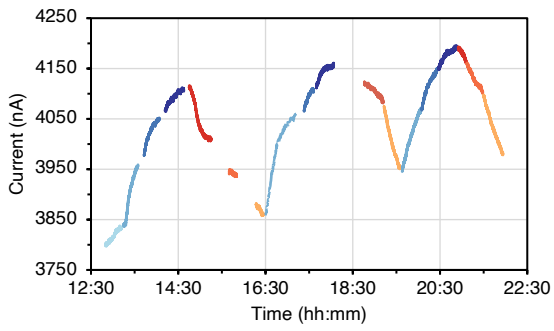
Blank (2)



Blank (2)



Blank (3)



Blank (3)

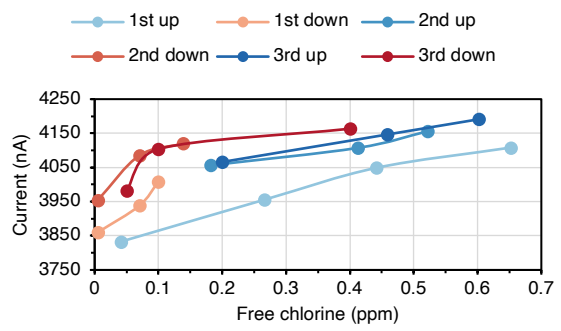


**Figure S6.** Replicate data from the real drinking water testing. The purple cross shows the sensor response to the real water, while the black crosses represent the sensor response to the spiked concentrations.

